ESTs, and identified 82 distinct transcripts (Tables 1 and 2, and supplementary Tables S1 and S2) in the FC and HPC that are relevant to LH and responsive to conventional antidepressants. To date, the strategy for designing antidepressive drugs is based on the serendipitous paradigm that the augmentation of monoaminergic activity in the central nervous system leads to therapeutic benefits.[1] However, currently available drugs have several drawbacks in terms of slow onset of action and intractable disease presents in approximately one-third of all depressive patients.[61] Given the genetically complex nature of human depression, we recognize that the present study can explain only limited aspects of depression pathology. Nevertheless, we believe that this study could give rise to new ideas for probing into the genetic mechanisms of human affective disorder and for refining the development of advanced therapeutics.

DUALITY OF INTEREST

None declared

ACKNOWLEDGEMENTS

We would like to thank Shuichi Tsutsumi and Hiroko Meguro for assistance with microarray data analysis, Yuichi Ishitsuka, Yuki Iijima and Shin-ichi Ohno for help with animal experiments, Kazuo Yamada for useful comments and Joanne Meerabux for critical reading of this manuscript. This study was partly supported by Grants-in-Aid for Young Scientists (B) (No. 13770566) from the Ministry of Education, Culture, Sports and Technology (MEXT).

ABBREVIATIONS

BDNF	*brain-derived neurotrophic factor*
EST	*expressed sequence tag*
FC	*frontal cortex*
HPC	*hippocampus*
IS	*inescapable shocks*
LH	*learned helplessness*
LH-F	*LH rats treated with fluoxetine*
LH-I	*LH rats treated with imipramine*
LH-S	*LH rats treated with saline*
NMDA	*N-methyl-D-aspartate*
NREM	*nonrapid eye movement*
PKC	*protein kinase C*
RT	*reverse transcription*
SSRI	*selective serotonin reuptake inhibitor*
TCA	*tricyclic antidepressant*

SUPPLEMENTARY INFORMATION

Supplementary Information accompanies the paper on the TPJ website (http://www.nature.com/tpj).

REFERENCES

1 Nestler EJ, Barrot M, DiLeone RJ, Eisch AJ, Gold SJ, Monteggia LM. Neurobiology of depression. *Neuron* 2002; **34**: 13–25.
2 Fava M, Kendler KS. Major depressive disorder. *Neuron* 2000; **28**: 335–341.
3 Detera-Wadleigh SD, Badner JA, Berrettini WH, Yoshikawa T, Goldin LR, Turner G *et al.* A high-density genome scan detects evidence for a bipolar-disorder susceptibility locus on 13q32 and other potential loci on 1q32 and 18p11.2. *Proc Natl Acad Sci USA* 1999; **96**: 5604–5609.
4 Overmier JB, Seligman ME. Effects of inescapable shock upon subsequent escape and avoidance responding. *J Comp Physiol Psychol* 1967; **63**: 28–33.
5 Telner JI, Singhal RL. Psychiatric progress. The learned helplessness model of depression. *J Psychiatr Res* 1984; **18**: 207–215.
6 Geoffroy M, Scheel-Kruger J, Christensen AV. Effect of imipramine in the 'learned helplessness' model of depression in rats is not mimicked by combinations of specific reuptake inhibitors and scopolamine. *Psychopharmacology* 1990; **101**: 371–375.
7 Nankai M, Yamada S, Muneoka K, Toru M. Increased 5-HT2 receptor-mediated behavior 11 days after shock in learned helplessness rats. *Eur J Pharmacol* 1995; **281**: 123–130.
8 Willner P. A Psychobiological Synthesis. In: *Depression.* John Wiley & Sons: New York 1985.
9 Ferguson SM, Brodkin JD, Lloyd GK, Menzaghi F. Antidepressant-like effects of the subtype-selective nicotinic acetylcholine receptor agonist, SIB-1508Y, in the learned helplessness rat model of depression. *Psychopharmacology* 2000; **152**: 295–303.
10 Sherman AD, Petty F. Learned helplessness decreases [^{3}H]imipramine binding in rat cortex. *J Affect Disord* 1984; **6**: 25–32.
11 Mac Sweeney CP, Lesourd M, Gandon JM. Antidepressant-like effects of alnespirone (S 20499) in the learned helplessness test in rats. *Eur J Pharmacol* 1998; **345**: 133–137.
12 Musty RE, Jordan MP, Lenox RH. Criterion for learned helplessness in the rat: a redefinition. *Pharmacol Biochem Behav* 1990; **36**: 739–744.
13 Drevets WC, Price JL, Simpson Jr JR, Todd RD, Reich T, Vannier M *et al.* Subgenual prefrontal cortex abnormalities in mood disorders. *Nature* 1997; **386**: 824–827.
14 Jacobs BL, Praag H, Gage FH. Adult brain neurogenesis and psychiatry: a novel theory of depression. *Mol Psychiatry* 2000; **5**: 262–269.
15 Malberg JE, Eisch AJ, Nestler EJ, Duman RS. Chronic antidepressant treatment increases neurogenesis in adult rat hippocampus. *J Neurosci* 2000; **20**: 9104–9110.
16 Eriksson PS, Perfilieva E, Bjork-Eriksson T, Alborn AM, Nordborg C, Peterson DA *et al.* Neurogenesis in the adult human hippocampus. *Nat Med* 1998; **4**: 1313–1317.
17 Martin P, Soubrie P, Simon P. The effect of monoamine oxidase inhibitors compared with classical tricyclic antidepressants on learned helplessness paradigm. *Progr Neuro-Psychopharmacol Biol Psychiatry* 1987; **11**: 1–7.
18 Nakagawa Y, Ishima T, Ishibashi Y, Tsuji M, Takashima T. Involvement of GABAB receptor systems in action of antidepressants. II: Baclofen attenuates the effect of desipramine whereas muscimol has no effect in learned helplessness paradigm in rats. *Brain Res* 1996; **728**: 225–230.
19 Nakagawa Y, Sasaki A, Takashima T. The GABA(B) receptor antagonist CGP36742 improves learned helplessness in rats. *Eur J Pharmacol* 1999; **381**: 1–7.
20 Tejedor-Real P, Mico JA, Maldonado R, Roques BP, Gibert-Rahola J. Implication of endogenous opioid system in the learned helplessness model of depression. *Pharmacol Biochem Behav* 1995; **52**: 145–152.
21 Anthony JP, Sexton TJ, Neumaier JF. Antidepressant-induced regulation of 5-HT(1b) mRNA in rat dorsal raphe nucleus reverses rapidly after drug discontinuation. *J Neurosci Res* 2000; **61**: 82–87.
22 Bristow LJ, O'Connor D, Watts R, Duxon MS, Hutson PH. Evidence for accelerated desensitisation of 5-HT_{2C} receptors following combined treatment with fluoxetine and the 5-HT_{1A} receptor antagonist, WAY 100,635, in the rat. *Neuropharmacology* 2000; **39**: 1222–1236.
23 Tordera RM, Monge A, Del Rio J, Lasheras B. Antidepressant-like activity of VN2222, a serotonin reuptake inhibitor with high affinity at 5-HT1A receptors. *Eur J Pharmacol* 2002; **442**: 63–71.
24 Mirnics K, Middleton AF, Lewis AD, Levitt P. Analysis of complex brain disorders with gene expression microarrays: schizophrenia as a disease of the synapse. *Trends Neurosci* 2001; **24**: 479–486.
25 Raychaudhuri S, Stuart JM, Altman RB. Principal components analysis to summarize microarray experiments: application to sporulation time series. *Pacific Symp Biocomput* 2000: 455–466.
26 Wurmbach E, Yuen T, Ebersole BJ, Sealfon SC. Gonadotropin-releasing hormone receptor-coupled gene network. *J Biol Chem* 2001; **276**: 47195–47201.
27 Papolos DF, Yu YM, Rosenbaum E, Lachman HM. Modulation of learned helplessness by 5-hydroxytryptamine2A receptor antisense oligodeoxynucleotides. *Psychiatr Res* 1996; **63**: 197–203.
28 Wu J, Kramer GL, Kram M, Steciuk M, Crawford IL, Petty F. Serotonin and learned helplessness: a regional study of 5-HT1A, 5-HT2A receptors

and the serotonin transport site in rat brain. *J Psychiatr Res* 1999; **33**: 17–22.
29 Pandey GN, Pandey SC, Dwivedi Y, Sharma RP, Janicak PG, Davis JM. Platelet serotonin-2A receptors: a potential biological marker for suicidal behavior. *Am J Psychiatry* 1995; **152**: 850–855.
30 Velbinger K, De Vry J, Jentzsch K, Eckert A, Henn F, Muller WE. Acute stress induced modifications of calcium signaling in learned helpless rats. *Pharmacopsychiatry* 2000; **33**: 132–137.
31 Aldenhoff JB, Dumais-Huber C, Fritzsche M, Sulger J, Vollmayr B. Altered Ca(2+)-homeostasis in single T-lymphocytes of depressed patients. *J Psychiatr Res* 1997; **31**: 315–322.
32 Hayaishi O. Molecular mechanisms of sleep–wake regulation: a role of prostaglandin D2. *Philos Trans R Soc London—Ser B Biol Sci* 2000; **355**: 275–280.
33 Mizoguchi A, Eguchi N, Kimura K, Kiyohara Y, Qu WM, Huang ZL *et al.* Dominant localization of prostaglandin D receptors on arachnoid trabecular cells in mouse basal forebrain and their involvement in the regulation of non-rapid eye movement sleep. *Proc Natl Acad Sci USA* 2001; **98**: 11674–11679.
34 Feng J, Cai X, Zhao J, Yan Z. Serotonin receptors modulate GABA(A) receptor channels through activation of anchored protein kinase C in prefrontal cortical neurons. *J Neurosci* 2001; **21**: 6502–6511.
35 Missler M, Hammer RE, Sudhof TC. Neurexophilin binding to alpha-neurexins. A single LNS domain functions as an independently folding ligand-binding unit. *J Biol Chem* 1998; **273**: 34716–34723.
36 Missler M, Sudhof TC. Neurexophilins form a conserved family of neuropeptide-like glycoproteins. *J Neurosci* 1998; **18**: 3630–3638.
37 Nunoue K, Ohashi K, Okano I, Mizuno K. LIMK-1 and LIMK-2, two members of a LIM motif-containing protein kinase family. *Oncogene* 1995; **11**: 701–710.
38 Sarmiere PD, Bamburg JR, Meng Y, Zhang Y, Tregoubov V, Janus C *et al.* Head, neck, and spines. A role for LIMK-1 in the hippocampus. Abnormal spine morphology and enhanced LTP in LIMK-1 knockout mice. *Neuron* 2002; **35**: 3–5.
39 Steffens DC, Krishnan KR. Structural neuroimaging and mood disorders: recent findings, implications for classification, and future directions. *Biol Psychiatry* 1998; **43**: 705–712.
40 Okano I, Hiraoka J, Otera H, Nunoue K, Ohashi K, Iwashita S *et al.* Identification and characterization of a novel family of serine/threonine kinases containing two N-terminal LIM motifs. *J Biol Chem* 1995; **270**: 31321–31330.
41 Altar CA. Neurotrophins and depression. *Trends Pharmacol Sci* 1999; **20**: 59–61.
42 Skolnick P. Antidepressants for the new millennium. *Eur J Pharmacol* 1999; **375**: 31–40.
43 Brandoli C, Sanna A, De Bernardi MA, Follesa P, Brooker G, Mocchetti I. Brain-derived neurotrophic factor and basic fibroblast growth factor downregulate NMDA receptor function in cerebellar granule cells. *J Neurosci* 1998; **18**: 7953–7961.
44 Gould E, Tanapat P. Stress and hippocampal neurogenesis. *Biol Psychiatry* 1999; **46**: 1472–1479.
45 McEwen BS. Stress and hippocampal plasticity. *Annu Rev Neurosci* 1999; **22**: 105–122.
46 McEwen BS. Effects of adverse experiences for brain structure and function. *Biol Psychiatry* 2000; **48**: 721–731.
47 Prince JA, Blennow K, Gottfries CG, Karlsson I, Oreland L. Mitochondrial function is differentially altered in the basal ganglia of chronic schizophrenics. *Neuropsychopharmacology* 1999; **21**: 372–379.
48 Maurer I, Zierz S, Moller H. Evidence for a mitochondrial oxidative phosphorylation defect in brains from patients with schizophrenia. *Schizophr Res* 2001; **48**: 125–136.
49 Jha N, Jurma O, Lalli G, Liu Y, Pettus EH, Greenamyre JT *et al.* Glutathione depletion in PC12 results in selective inhibition of mitochondrial complex I activity. Implications for Parkinson's disease. *J Biol Chem* 2000; **275**: 26096–26101.
50 Chinopoulos C, Adam-Vizi V. Mitochondria deficient in complex I activity are depolarized by hydrogen peroxide in nerve terminals: relevance to Parkinson's disease. *J Neurochem* 2001; **76**: 302–306.
51 Volz HP, Rzanny R, Riehemann S, May S, Hegewald H, Preussler B *et al.* 31P magnetic resonance spectroscopy in the frontal lobe of major depressed patients. *Eur Arch Psychiatr Clin Neurosci* 1998; **248**: 289–295.
52 Jaksch M, Lochmuller H, Schmitt F, Volpel B, Obermaier-Kusser B, Horvath R. A mutation in mt tRNALeu(UUR) causing a neuropsychiatric syndrome with depression and cataract. *Neurology* 2001; **57**: 1930–1931.
53 Kato T. The other, forgotten genome: mitochondrial DNA and mental disorders. *Mol Psychiatry* 2001; **6**: 625–633.
54 Yoshikawa T, Kikuchi M, Saito K, Watanabe A, Yamada K, Shibuya H *et al.* Evidence for association of the myo-inositol monophosphatase 2 (IMPA2) gene with schizophrenia in Japanese samples. *Mol Psychiatry* 2001; **6**: 202–210.
55 Schwab SG, Hallmayer J, Lerer B, Albus M, Borrmann M, Honig S *et al.* Support for a chromosome 18p locus conferring susceptibility to functional psychoses in families with schizophrenia, by association and linkage analysis. *Am J Hum Genet* 1998; **63**: 1139–1152.
56 Kroczka B, Branski P, Palucha A, Pilc A, Nowak G. Antidepressant-like properties of zinc in rodent forced swim test. *Brain Res Bull* 2001; **55**: 297–300.
57 Maes M, Vandoolaeghe E, Neels H, Demedts P, Wauters A, Meltzer HY *et al.* Lower serum zinc in major depression is a sensitive marker of treatment resistance and of the immune/inflammatory response in that illness. *Biol Psychiatry* 1997; **42**: 349–358.
58 Quackenbush J. Computational analysis of microarray data. *Nat Rev Genet* 2001; **2**: 418–427.
59 Steingard RJ, Renshaw PF, Hennen J, Lenox M, Cintron CB, Yuoung AD *et al.* Smaller frontal lobe white matter volumes in depressed adolescents. *Biol Psychiatry* 2002; **52**: 413–417.
60 Cowan WM, Kopnisky KL, Hyman SE. The human genome project and its impact on psychiatry. *Annu Rev Neurosci* 2002; **25**: 1–50.
61 Skolnick P, Legutko B, Li X, Bymaster FP. Current perspectives on the development of non-biogenic amine-based antidepressants. *Pharmacol Res* 2001; **43**: 411–423.
62 Crescenzi M, Giuliani A. The main biological determinants of tumor line taxonomy elucidated by a principal component analysis of microarray data. *FEBS Lett* 2001; **507**: 114–118.
63 Landgrebe J, Welzl G, Metz T, van Gaalen MM, Ropers H, Wurst W *et al.* Molecular characterization of antidepressant effects in the mouse brain using gene expression profiling. *J Psychiatr Res* 2002; **36**: 119–129.

Journal of Cerebral Blood Flow & Metabolism
24:212–223 © 2004 The International Society for Cerebral Blood Flow and Metabolism
Published by Lippincott Williams & Wilkins, Inc., Baltimore

Genome-wide Gene Expression Analysis for Induced Ischemic Tolerance and Delayed Neuronal Death Following Transient Global Ischemia in Rats

*§Nobutaka Kawahara, *Yan Wang, *†Akitake Mukasa, *§Kazuhide Furuya, ‖Tatsuya Shimizu, ‡Takao Hamakubo, †Hiroyuki Aburatani, ‡Tatsuhiko Kodama, and *§Takaaki Kirino

**Department of Neurosurgery, Faculty of Medicine, University of Tokyo, Japan; †Genomescience and ‡Molecular Biology Divisions, Research Center for Advanced Science and Technology, University of Tokyo, Japan; §SORST (Solution-Oriented Research for Science and Technology), Japan Science and Technology Cooperation (JST), Saitama, Japan; and ‖Department of Neurosurgery, Gunma University School of Medicine, Japan.*

Summary: Genome-wide gene expression analysis of the hippocampal CA1 region was conducted in a rat global ischemia model for delayed neuronal death and induced ischemic tolerance using an oligonucleotide-based DNA microarray containing 8,799 probes. The results showed that expression levels of 246 transcripts were increased and 213 were decreased following ischemia, corresponding to 5.1% of the represented probe sets. These changes were divided into seven expression clusters using hierarchical cluster analysis, each with distinct conditions and time-specific patterns. Ischemic tolerance was associated with transient up-regulation of transcription factors (c-Fos, JunB Egr-1, -2, -4, NGFI-B), Hsp70 and MAP kinase cascade-related genes (MKP-1), which are implicated cell survival. Delayed neuronal death exhibited complex long-lasting changes of expression, such as up-regulation of proapoptotic genes (GADD153, Smad2, Dral, Caspase-2 and -3) and down-regulation of genes implicated in survival signaling (MKK2, and PI4 kinase, DAG/PKC signaling pathways), suggesting an imbalance between death and survival signals. Our study provides a differential gene expression profile between delayed neuronal death and induced ischemic tolerance in a genome-wide analysis, and contributes to further understanding of the complex molecular pathophysiology in cerebral ischemia.
Key Words: global ischemia—hippocampus—delayed neuronal death—ischemic tolerance—DNA microarray—gene expression.

Transient cerebral ischemia causes selective and delayed neuronal death in the vulnerable hippocampal CA1 region (Kirino 1982; Pulsinelli et al., 1982). Since this type of neuronal death occurs over several days, suggesting a potentially wide therapeutic window, its pathophysiological mechanisms have been intensively investigated as a model of ischemic neuronal injury. Various studies have provided evidence that cerebral ischemia induces transcriptional activation of a variety of genes (MacManus and Linnik 1997), particularly those related to stress response, cell death or survival (Chen et al., 1996; Chen et al., 1997; Chen et al., 1998; Nowak 1990), suggesting a close relationship with neuronal ischemic vulnerability. Based on these observations, various attempts have been made to identify differentially expressed mRNA by using subtractive hybridization (Wang et al., 2001) and PCR based techniques (Schwarz et al., 2002), which were expected to elucidate the complex molecular events leading to ischemic neuronal death. Despite these efforts, the underlying pathophysiological mechanisms remain unknown.

Recent advances in DNA microarray technology have provided tools to analyze the expression of thousands of genes in a single hybridization experiment (Lockhart and Winzeler 2000). In cerebral ischemia, this approach has been used to uncover key molecular events using a focal ischemia model (Keyvani et al., 2002; Kim et al., 2002; Raghavendra Rao et al., 2002; Soriano et al., 2000), and global ischemia or hypoxic models (Bernaudin et al., 2002; Jin et al., 2001). These studies, however, have limitations in evaluating global and sequential changes in gene expression related to cell death or survival, due to restricted time points, limited and biased transcripts represented on the array, and the nature of the sample analyzed.

Received June 12, 2003; accepted October 20, 2003.
This study was supported in part by a Grant-in-Aid from the Ministry of Education, Culture, Sports, Science and Technology, Japan, and by the Mitsubishi Foundation.
Address correspondence and reprint requests to N. Kawahara, Department of Neurosurgery, Faculty of Medicine, University of Tokyo, 7–3-1, Hongo, Bunkyo-ku, Tokyo, 113–8655, Japan; e-mail:kawahara-tky@umin.ac.jp

DOI: 10.1097/01.WCB.0000106012.33322.A2

Our study was designed to demonstrate global and sequential changes of gene expression during the process of ischemic neuronal death in the hippocampus. For this, we specifically analyzed a microdissected hippocampal CA1 region one to 48 hours after ischemia using an oligonucleotide-based DNA microarray containing approximately 7,000 full-length known or annotated genes and 1,000 EST clusters. We compared these changes with those during the induction of ischemic tolerance. It is widely known that hippocampal neurons can acquire resistance to ischemia when subjected to sublethal ischemia several days prior to lethal ischemia (for review, refer to Kirino, 2002). Comparison of global expression profiles during the process of ischemic cell death and ischemic tolerance, should lead to a better understanding of the molecular pathophysiology of ischemia.

MATERIALS AND METHODS

Animals

The experiments were performed on male Wistar SPF rats (280–320 g, Charles River, Yokohama, Japan). All animal-related procedures were conducted in accordance with guidelines for the care and use of laboratory animals set out by the National Institutes of Health.

Experimental Groups

Four groups of animals were used. In the first experiment (single ischemia experiment), histological assessment of global cerebral ischemia in the hippocampal CA1 sector was performed in rats subjected to sham operation (n = 6), two-minute (n = 8) or six-minute (n = 10) ischemia. In the second experiment (double ischemia experiment), induction of ischemic tolerance by two-minute ischemia was evaluated. In this group, rats were preconditioned by either sham operation with vertebral artery coagulation (n = 10) or two-minute ischemia (n = 10), and then subjected to six-minute ischemia three days later. The hippocampus was then examined as in the previous experiment. In the third experiment, samples of hippocampal CA1 sector of the animals subjected to sham operation (n = 15), two-minute (n = 30) or six-minute ischemia (n = 30) were analyzed for global mRNA expression (GeneChip experiment). In the final group, rats were subjected to sham, two-minute, or six-minute ischemia, and then sacrificed for *in situ* hybridization study.

Global Cerebral Ischemia

Global cerebral ischemia was induced by a modification of the four-vessel occlusion method (Pulsinelli et al., 1982). Rats were fixed in a stereotaxic frame under 1% halothane anesthesia. Both vertebral arteries were exposed under a microscope by drilling through the foramina, then coagulated and completely cut using fine-tipped bipolar forceps. Twelve hours later, under fasting conditions, the animals were intubated and put on a rodent respirator (Model 7025, Ugo Basile, Comerio, Italy) under 1.0% halothane anesthesia in a 30% O_2/ 70% N_2O mixture. The left femoral artery and vein were cannulated for blood pressure (BP) monitoring (Carrier Amplifier AP-601G, Nihon Kohden, Tokyo, Japan) and intravenous drug administration. The right femoral artery was also cannulated for exsanguination. Atropine sulfate (0.25mg/kg, ip) and amikacin (10mg/kg, ip) were administered. Rectal temperature was maintained at 37.5°C using a heating blanket (Animal Blanket Controller, Model ATB-1100, Nihon Kohden) for 30 minutes postischemia. Temporal muscle temperature was monitored with a thermometer (Model BAT-12, Physitemp Instruments, Clifton, NJ, USA) via a needle microprobe (MT-26/2, Physitemp Instruments) and kept at 37°C with a heating lamp. Cerebral ischemia was induced for either 2 or 6 minutes by occluding the bilateral common carotid arteries with clips. During ischemia, BP was lowered to 60 mmHg by exsanguination into a heparinized syringe from the right femoral artery, and electrical silence was confirmed by electroencepalogram (EEG) with needle electrodes connected to an amplifier (Bioelectric Amplifier AB-621G, Nihon Kohden, Tokyo, Japan). Following reperfusion, all physiological parameters were controlled for 30 minutes, and the animals were returned to their cages after extubation. Arterial blood samples were analyzed before, five, and 30 minutes after ischemia using a blood gas analyzer (Model 248, Chiron Diagnostics Ltd., Essex, UK) and a glucose analyzer (Glu-1, TOA Electronics Ltd., Tokyo, Japan). During the procedure, PaO_2 was maintained at 120–140 mmHg by adjusting inhaled O_2 concentration, and $PaCO_2$ at 35–40 mmHg by changing the respiratory rate. Base excess was corrected by intravenous injection of sodium bicarbonate and kept at −2.0 to 2.0 mEq/L. Sham operated animals were similarly treated except for vertebral artery coagulation and carotid artery clipping. In the double ischemia group (tolerance experiment), vertebral artery coagulation was performed in the sham operation.

Histological Assessment of Ischemic Neuronal Injury

Seven days after ischemia or sham operation, the animals were put under 2% halothane anesthesia and then fixed by transcardiac perfusion with 4% paraformaldehyde in 0.1mol/L phosphate buffer (pH = 7.4). The brains were left *in situ* for three hours, removed, and post-fixed overnight at 4°C, then embedded in paraffin. Coronal sections (4-μm thickness) obtained from the dorsal hippocampus (approximately 3.8 mm from bregma) (Paxinos and Watson 1986) were stained with hematoxylin and eosin, and the number of intact neurons was counted in a blind fashion along the pyramidal layer of the CA1 sector for 1 mm. The neuronal densities obtained (cells/mm) were averaged for each hemisphere and compared. In the first single ischemia group, one-way analysis of variance (ANOVA) with significance set at $p<0.05$ was used. In the second group (double ischemia), two-tailed unpaired Student's t-test with significance set at $p<0.05$ was used. All the data was shown as mean ±SD.

Microarray Experiment

Rats were subjected to sham operation, two-minute or six-minute ischemia, then sacrificed by decapitation under deep pentobarbital anesthesia at 1, 3, 12, 24, and 48 hours. The brains were quickly removed, frozen in 2-methylbutane at −20°C, and stored at −80°C. The brains were cut into 2-mm coronal sections and the dorsal hippocampal CA1 sector was dissected, under a microscope, at −20°C. Total RNA was extracted from pooled samples obtained from three rats using Isogen reagent (NipponGene Inc, Toyama, Japan), following the manufacturer's protocols. The quality of total RNA was verified by gel electrophoresis and $OD_{260/280nm}$ ratios.

Five micrograms of total RNA from each sample was used to synthesize biotin-labeled cRNA, which was then hybridized to a high-density oligonucleotide array (GeneChip Rat RG-U34A

array; Affymetrix Inc., Santa Clara, CA, USA), following a previously published protocol with minor modifications (Ishii et al., 2000). This array contains 8,799 probe sets derived from full-length or annotated genes (7,000 genes) as well as 1,000 EST clusters, which were selected from the Unigene Build 34, Genbank 110, and the dbEST databases. After washing, arrays were stained with streptavidin-phycoerythrin (Molecular Probes, Inc., Eugene, OR, USA) and analyzed by a Hewlett-Packard Scanner to collect primary data. The GeneChip 3.3 software (Affymetrix) was used to calculate the average difference for each gene probe on the array, which was shown as an intensity value of gene expression, defined by Affymetrix, using the proprietary algorithm. The average difference has been shown to quantitatively reflect the abundance of a particular mRNA molecule in a population (Ishii et al., 2000; Lockhart et al., 1996). To allow comparisons between multiple arrays, the average differences were normalized for each array by assigning the average of overall average difference values to be 100. A value of 20 was assigned to all average differences below 20.

Duplicate measurements were conducted for the two-minute and six-minute ischemia groups at each time point, and for the normal control group. For the sham-operated controls, a single RNA sample was evaluated at each time point. The resultant data was transferred to a database (Filemaker Pro 5, FileMaker, Inc., Santa Clara, CA, USA) and linked to Internet genome databases. To select genes with altered expression patterns, each data array obtained after ischemia was compared with those from the normal, time-matched, sham controls. The criterion of two-fold changes in the average difference for each probe set was used. To further increase the reproducibility, both duplicate samples must have met the two-fold change criteria for the data to be considered. The resultant data was transferred to GeneSpring 4.2 (SiliconGenetics, Redwood City, CA, USA) for hierarchical cluster analysis (Eisen et al., 1998). The most recent information for each transcript was obtained from databases such as Genbank, dbEST, Unigene, and the functional annotation was supplemented by protein database Swiss-Prot.

In Situ Hybridization

Five genes (Egr-2, TIEG, Homer-1C, BTG2, Caspase-2) that showed increased expression levels were chosen for this experiment. Total RNA obtained from normal adult rat brain, as described above, was subjected to RT–PCR using Ready-To-Go T-Primed First-Strand Kit (Amersham Biosciences, Buckinghamshire, UK) and Amplitaq Gold (Applied Biosystems, Foster City, CA, USA) according to the manufacturer's protocols. Sense and antisense PCR primers (22mers) were designed to amplify a fragment of Egr-2 (Accession No: U78102, 1821–2351, 531bp), TIEG (Accession No: U88630, 358–807, 450bp), Homer-1C (Accession No: AF030088, 1852–2332, 480bp), BTG2 (Accession No: M60921, 1861–2294, 434bp), and Caspase-2 (Accession No: U77933, 1641–2163, 470bp). PCR was conducted for 43 cycles (94°C for 30 seconds, 60°C for one minute, 72°C for one minute), and the obtained PCR fragments were subcloned into pPCR-Script Amp SK(+) (Stratagene, La Jolla, CA, USA). Orientation and sequence were verified by direct sequencing. Antisense and sense RNA probes were prepared from each cDNA using RNA labeling kit (Riboprobe Combination System-T3/T7, Promega, Madison, WI, USA) with T7 and T3 RNA polymerases. The probes were labeled by [α-^{35}S]-UTP (Amersham Biosciences) to a specific activity of approximately 1–2 $\times$ 10^6 cpm/ng.

The animals were sacrificed 1, 3, 12, 24, and 48 hours after ischemia under deep anesthesia with 4% halothane, the brains were immediately removed, frozen in powdered dry ice, and cut into 14 μm-thick coronal sections approximately 3.8 mm from bregma (Paxinos and Watson 1986) using a cryostat at –16°C. *In situ* hybridization was performed as previously described (Kawahara et al., 1999). Briefly, sections postfixed with 4% paraformaldehyde were hybridized with each cRNA probe at 55°C for 16 hours at a concentration of 1.0×10^4 cpm/μl. The next day, high stringency washes at 55°C were followed by RNase A treatment and dehydration. The sections were exposed, with a radioactive standard strip, to BioMax MR film (Eastman Kodak, Rochester, NY, USA) for 3–7 days.

RESULTS

Delayed Neuronal Death and Induction of Tolerance

In the first experiment, ischemic neuronal injury in the hippocampal CA1 sector was examined (Fig. 1). The CA1 neurons were significantly reduced only in the six-minute ischemia group (9.7 ±2.9% of normal control, $p<0.0001$ by ANOVA, with Bonferroni's post-hoc test) compared with those in the sham (90.3 ±6.8%) and two-minute (91.3 ±12.6%) groups. This observation indicates that, in our rat global ischemia model, six-minute ischemia is sufficient to induce severe hippocampal neuronal death, whereas two-minute ischemia does not cause any detectable injury. In the double ischemia experiment (Fig. 1), rats were subjected to either sham operation or two-minute ischemia three days prior to six-minute ischemia, and then sacrificed seven days later. Evaluation of hippocampal neuronal injury demonstrated that preconditioning via two-minute ischemia significantly protected CA1 neurons against subsequent six-minute ischemia (27.2 ±17.5% in sham and 80.6 ±8.8% with two-minute preconditioning, $p<0.0001$ by unpaired t-test), which confirmed the belief that short sublethal ischemia, provided by two-minute ischemia in our model, induced ischemic tolerance at three days.

Global Changes in mRNA Expression following Ischemia

Of 8,799 probe sets represented on the chip, 3,518 transcripts (40%) were considered present in normal controls according to the manufacturer's default computer algorithm. Of these, 238 transcripts, which correspond to 2.7% of the total probe set, were increased after ischemia compared with normal and time-matched sham controls using our current criteria (Fig. 2). In this group, 36 transcripts were increased following two-minute ischemia, and 224 transcripts following six-minute ischemia, while 22 transcripts were increased in both conditions. Similar analysis for decreased expression showed that 205 transcripts were down regulated following ischemia (2.3% of the total probe set), which was similar to the number of increased expression. Eight transcripts showed both up and down-regulation during their time course, giving a total of 451 transcripts (5.1% of the total probe set) that exhibited significant changes following ischemia. These were subjected to further analysis.

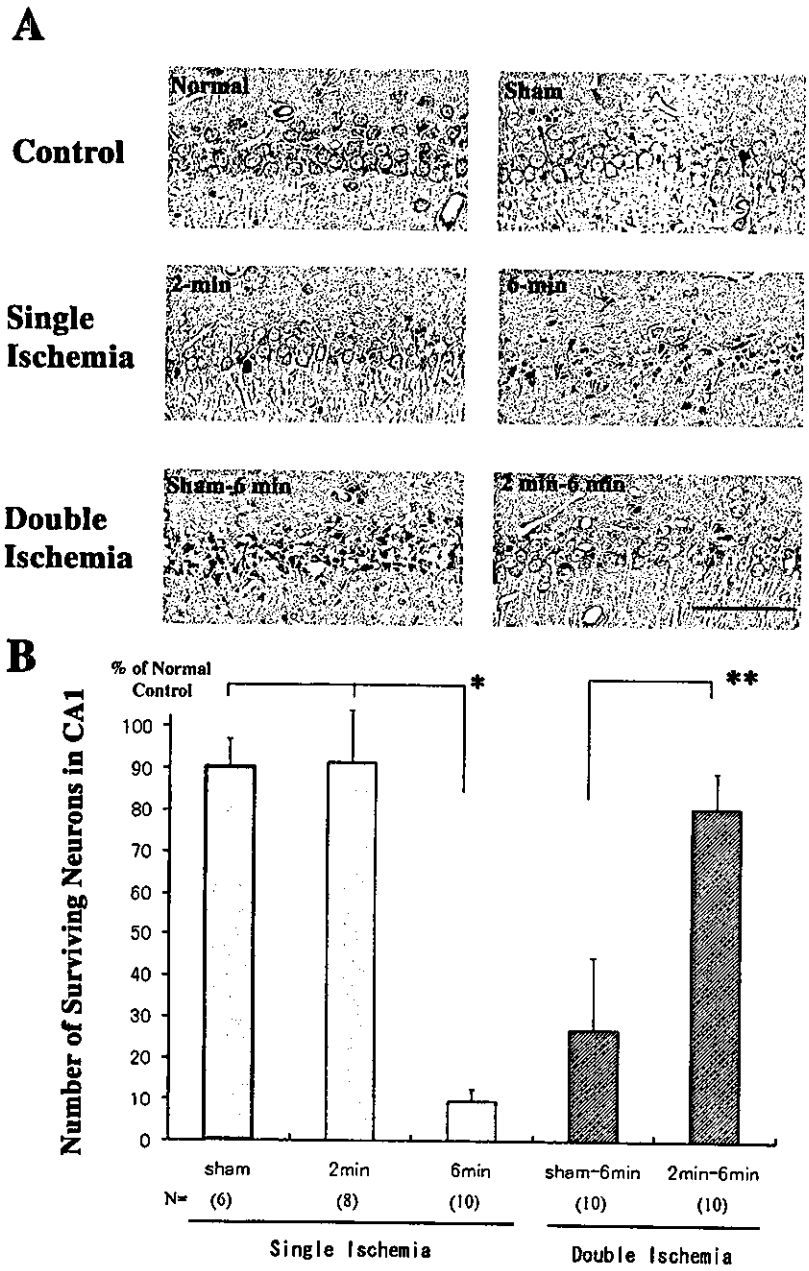

FIG. 1. A. Histological outcome in the CA1 sector of the hippocampus after single (two- and six-minute) and double (sham and six-minute, two- and six-minute) ischemia. Single short ischemia (two-minute) did not cause significant cell injury, while longer six-minute ischemia led to uniform severe neuronal death. Prior pretreatment with two-minute ischemia remarkably protected pyramidal neurons against otherwise lethal six-minute ischemia. Hematoxylin and eosin staining. Scale bar: 100 μm. B: Bar graph showing the density of intact neurons in the CA1 sector in each group, presented as % of normal control (mean ±SD).

Hierarchical Cluster Analysis for Coordinated Changes in mRNA Expression

To analyze the patterns of coordinated mRNA expression, we applied hierarchical cluster analysis (Eisen et al., 1998) to the transcripts with altered expression levels and could categorize these into seven clusters. As shown in Fig. 3, each cluster displayed distinctive time- and condition-specific characteristics. Transcripts included in cluster 2 showed immediate transient increases after both two- and six-minute ischemia, and corresponded to the majority of the up-regulated genes in two-minute ischemia, which overlap with a subset of those in six-minute ischemia. Specific changes in six-minute ischemia were shown in clusters 1 and 7, where these transcripts exhibited delayed increase or decrease, respectively. The transcripts in cluster 4 were markedly increased solely after six-minute ischemia. To analyze what type of transcripts are in each expression cluster, we searched nucleic acid databases, deleted duplicate transcripts of the same gene, and grouped each transcript into 20 functional categories. However, we could not find specific functional groups in the majority of clusters (data not shown), except clusters 2 and 4, which were highly specific for signal transducers/transcription factors and heat shock proteins, respectively.

Comparison of mRNA Expression between Ischemic Tolerance and Neuronal Death

To analyze differential expression profiles between two- and six-minute ischemia, genes with altered levels

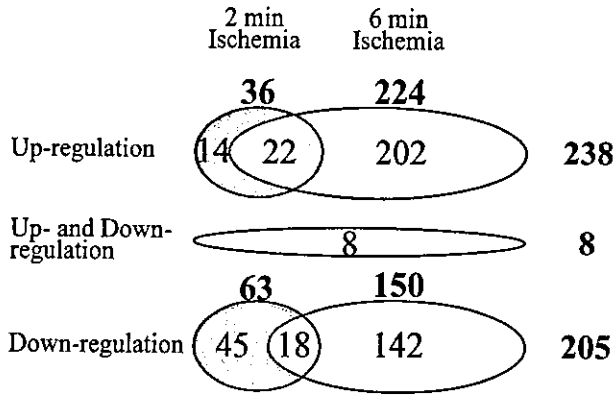

FIG. 2. Diagram showing the number of gene transcripts, up or down-regulated, after either two- or six-minute ischemia. Changes after two-minute ischemia are depicted in blue, those after six-minute in yellow, and those with overlapping transcripts in green. The transcripts showing both up and down-regulation during their time course are included in a separate circle in red.

of expression were compared according to their functional categories. The main results are shown in Fig. 4; some of the individual genes are listed in the Table and Fig. 5. The complete data set for individual transcripts is available at our web site (http://www2.genome.rcast.u-tokyo.ac.jp/egl/index_e.html).

Following two-minute ischemia, the majority of up-regulated genes are transcription factors, signal transducers, receptors, heat shock proteins, and cell cycle proteins. Among the transcription factors, leucine zipper transcription factors (c-Fos, JunB), zinc finger Egr family members, such as Egr-1 (NGFI-A, Krox24, zif268), Egr-2, Egr-4 (NGFI-C), and the closely related nuclear orphan receptor NGFI-B (Nurr77), showed increased expression. A marked up-regulation of mitogen-activated protein kinase phosphatases (MKP-1 and -3) was observed. In particular, MKP-1 showed a 10-fold increase in gene expression after two-minute ischemia. With regard to heat shock proteins, only HSP70 was up-regulated.

Following six-minute ischemia, several distinctive features were noted compared with those in two-minute ischemia, although similar up-regulation within the same functional categories was observed. Transcription factors related to cell death and growth arrest (KLF4, RNF4, GADD153, Smad2, NFκ b), signal transducers for cyclic AMP signaling (CAP1, PKI, ARPP-12, PDE4A), and proapoptotic factors (Dral, Caspase 2 and 3) were specifically increased after six-minute ischemia. Secondly, various heat shock proteins were increased, such as Hsp60, Hsp40, Hsp32, Hsp27, in addition to Hsp70. Finally, a substantial number of genes belonging to various functional groups were down-regulated. Of particular interest among these are signal transducers related to MAP kinase pathways (MKK2) and phosphatidyl inositol signaling (PI3 kinase, PI4 kinase), diacylglycerols (diacylglycerol kinase-2, -3, -6), protein kinase C (PKC β and γ), calcium/calmodulin dependent protein kinase (CAMK II α and β) and calcium signaling (IP3 kinase, IP3 receptor). In addition to these, glutamate receptors of various types, such as AMPA-type (GluR-1, -2, -3), NMDA-type (NMDAR1, NMDAR2A), and metabotropic type (mGluR3), were also down-regulated, as well as TGF beta receptor.

In Situ Hybridization

To confirm the microarray data, we selected five genes from four different categories that showed increased expression and performed *in situ* hybridization study. For each gene, the autoradiographs at the peak value in the microarray experiment are shown in Fig. 6. Egr-2 (a transcription factor), TIEG (TGF inducible early growth response protein), and Homer-1C (a postsynaptic membrane protein) showed early increase in both two- and six-minute ischemia in the microarray experiment. These increases were confirmed in the CA1 pyramidal layer by *in situ* hybridization for Egr-2 and Homer-1C. However, the hybridization signal in TIEG was equivocal. BTG2 (B-cell translocation gene 2) and Caspase-2 showed increased expression only after six-minute ischemia, which were also confirmed by *in situ* hybridization. Thus, time-course and condition-specific alterations of mRNA expression were confirmed for four out of five genes.

DISCUSSION

We used a nonbiased oligonucleotide-based DNA microarray to assess alterations in gene expression after ischemia in the hippocampal CA1 region, where ischemic cell death and tolerance are specifically demonstrated. Of a total of 8,799 transcripts surveyed, 3,518 transcripts (40.0%) were present in normal conditions and 451 (5.1%) exhibited distinct changes following ischemia. Among these, ischemic tolerance was associated with changes in only 1.2% of the total transcripts, whereas ischemic cell death induced changes in 4.5%. This ratio is consistent with other studies which demonstrated changes in 0.6–2.0% of genes screened in physiological conditions such as aging (Lee et al., 2000) and environmental enrichment (Rampon et al., 2000), while pathological conditions were associated with a greater number of changes ranging from 6 to 10% (Friddle et al., 2000; Song et al., 2001; Stanton et al., 2000). In this regard, our study confirmed the idea that cellular injury is associated with greater changes in gene expression when compared with those in cellular adaptation to the same insult, in our case, ischemia.

A major obstacle in expression profiling by DNA microarray technology has been how to analyze a huge data set to obtain indicative information underlying a specific condition. We used hierarchical cluster analysis, which can efficiently group together the transcripts with similar

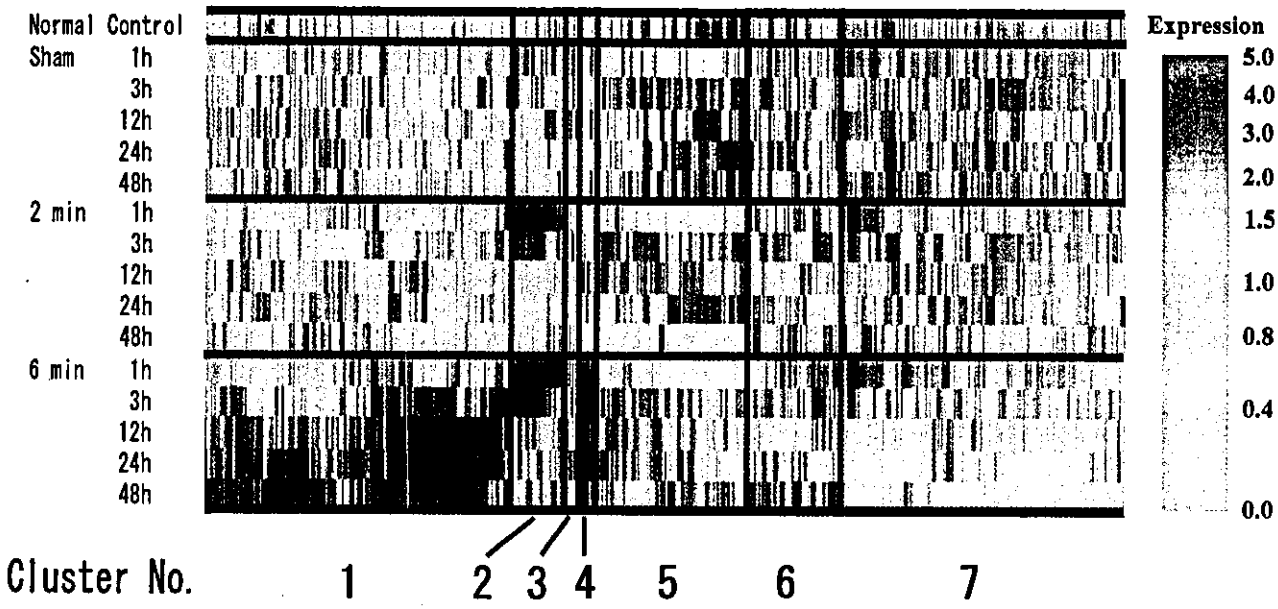

FIG. 3. Clustered gene expression patterns of 451 transcripts that displayed differential expression in two- or six-minute ischemia by hierarchical cluster analysis. Each column represents an individual transcript and the row pertains to different data sets collected at different conditions and times as indicated. Genes with similar patterns of changes were grouped into seven clusters with distinct time and condition-specific features.

changes by pairwise, average-linkage cluster analysis (Eisen et al., 1998). This approach revealed condition-specific changes, for example, that six-minute ischemia induced delayed and long-lasting changes compared with two-minute ischemia, as demonstrated by clusters 1 and 7. This clearly indicates that lethal ischemia initiates more complex, long-lasting cascades of molecular events. Although this approach is expected to produce similar functional groups (Lockhart and Winzeler 2000), we did not observe specific correlation, except for

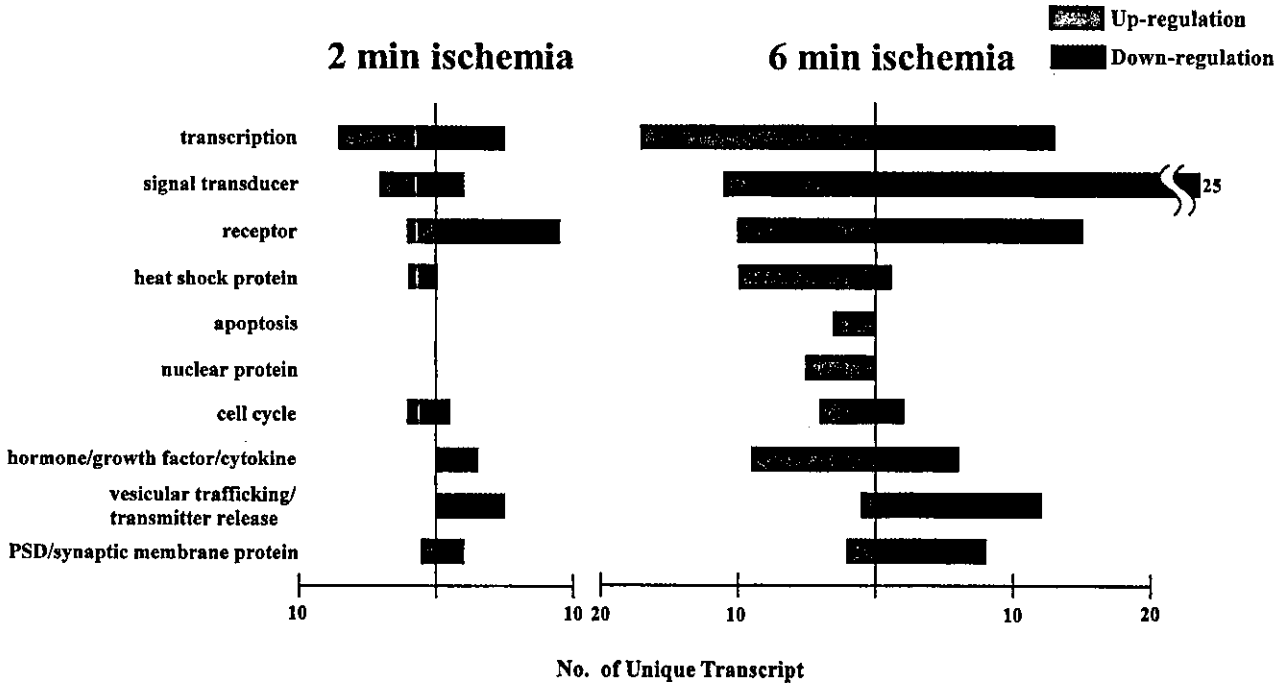

FIG. 4. Bar diagram showing the numbers of transcripts in 10 major functional categories that exhibited up and down-regulation after two- and six-minute ischemia. Some categories, such as transcription, signal transducer, and heat shock proteins exhibited similar patterns, whereas apoptosis proteins, nuclear proteins, and hormone/growth factor/cytokine groups were more specifically altered after six-minute ischemia.

TABLE 1. *List of genes in relation to ischemia*

Genbank accession no	Gene name	Normal control	Peak changes (fold)				Cluster no
		Average signal	2 minutes		6 minutes		
			Increase	Decrease	Increase	Decrease	
Transcription							
X06769	c-fos	20	7.70		17.26		2
U78102	EGR-2 (KROX20)	31	4.84		7.45		2
X54686	Jun-B	34	3.44		4.38		2
AI172476	TGF-beta inducible early growth response (Tieg)	39	2.78		5.37		1
U75397	EGR-1 (NGFI-A, KROX24)	410	2.66		3.29	0.32	7
M92433	EGR-4 (NGFI-C)	141	2.61		3.33		2
U17254	NGFI-B (Nurr77)	271	2.13		2.19		7
L26292	Kruppel-like factor 4 (KLF4)	20			7.19		2
AF022081	Ring finger protein 4 (RNF4), SNURF	21			3.85		5
U30186	GADD153	27			2.95		1
AB017912	Smad 2	30			2.55		1
L26267	NF kappa b p105 subunit	35			2.24		1
Signal transducer							
U02553	MAP kinase phosphatase 1(MKP-1)	20	10.58		14.14		2
X94185	MAP kinase phosphatase 3 (MKP-3)	165	2.30	0.23	2.97		2
L11930	Adenylyl cyclase-associated protein 1(CAP1)	119		0.44			1
L02615	cAMP-dependent protein kinase inhibitor (PKI)	26			3.29		1
S65091	cAMP-regulated phosphoprotein, ARPP-21	32			2.55		1
M26715	cAMP-dependent phosphodiesterase (PDE4A)	50			2.35	0.40	7
L14936	MAP kinase kinase (MKK2)	152				0.21	5
X07287	PKC gamma	443				0.21	7
X56917	IP3 3-kinase	596				0.25	7
U38812	IP3 receptor	67				0.30	7
M16960	CAMK II, alpha chain	86				0.31	7
D832538	PI 4-kinase, 230kDa	91				0.33	7
AA818983	Diacylglycerol kinase-2	52				0.38	5
D38448	Diacylglycerol kinase-3	84				0.39	7
D64046	PI3-kinase p85 beta subunit	61				0.39	7
K03486	PKC beta	413				0.40	7
M16112	CAMK II, beta chain	1269				0.41	7
D78588	Diacylglycerol kinase-6	1090				0.48	7
Receptor							
M36419	Glutamate receptor (GluR-2)	347		0.27			5
M92076	Metabotropic glutamate receptor 3 (mGluR-3)	385		0.35			5
M36420	Glutamate receptor (GluR-3)	45		0.45		0.45	5
M77809	TGF-beta receptor type 3	104				0.19	7
M36418	Glutamate receptor (GluR-1)	161				0.22	7
U11418	Glutamate receptor (NMDAR1)	86				0.32	7
AF001423	Glutamate receptor (NMDAR2A)	47				0.43	7
Heat shock protein							
Z75029	Heat shock protein 70	20	10.48		133.88		4
AA998683	Heat shock protein 27	21			71.64		1
U68562	Heat shock protein 60	133			8.38		1
AI170613	Heat shock protein 10	322			5.13		1
AA800551	Heat shock protein 40 (DnaJ-like protein)	345			4.08		1
AI179610	Heat shock protein 32 (heme oxygenase)	52			3.93		1
Apoptosis							
U77933	Caspase 3	20			2.99		1
U49930	Caspase 3	21			2.66		1
AA891527	Dral	161			2.28		1
Cell cycle							
AF030091	cyclin ania-6a	23	5.49		6.39		1
D14014	Cyclin D1	20	3.46				5
M60921	B-cell translocation gene 2 (BTG2)	30			5.43		2
PSD, synaptic membrane protien, vesicular trafficking/transmitter release							
AF030088	Homer-1C (PSD-ZIP45)	29	2.97		11.51		2

clusters 2 and 4 which were mostly specific to signal transducer/transcription factors and heat shock proteins, suggesting limitation of this assumption in ischemia.

One of the main purposes of our study was to find key molecular events leading to ischemic tolerance and delayed neuronal death by global expression monitoring. This approach is based on the hypothesis that the abundance of RNA is proportional to the amount of protein. After lethal ischemia, it is known that translational activity is significantly decreased (Kleihues and Hossmann

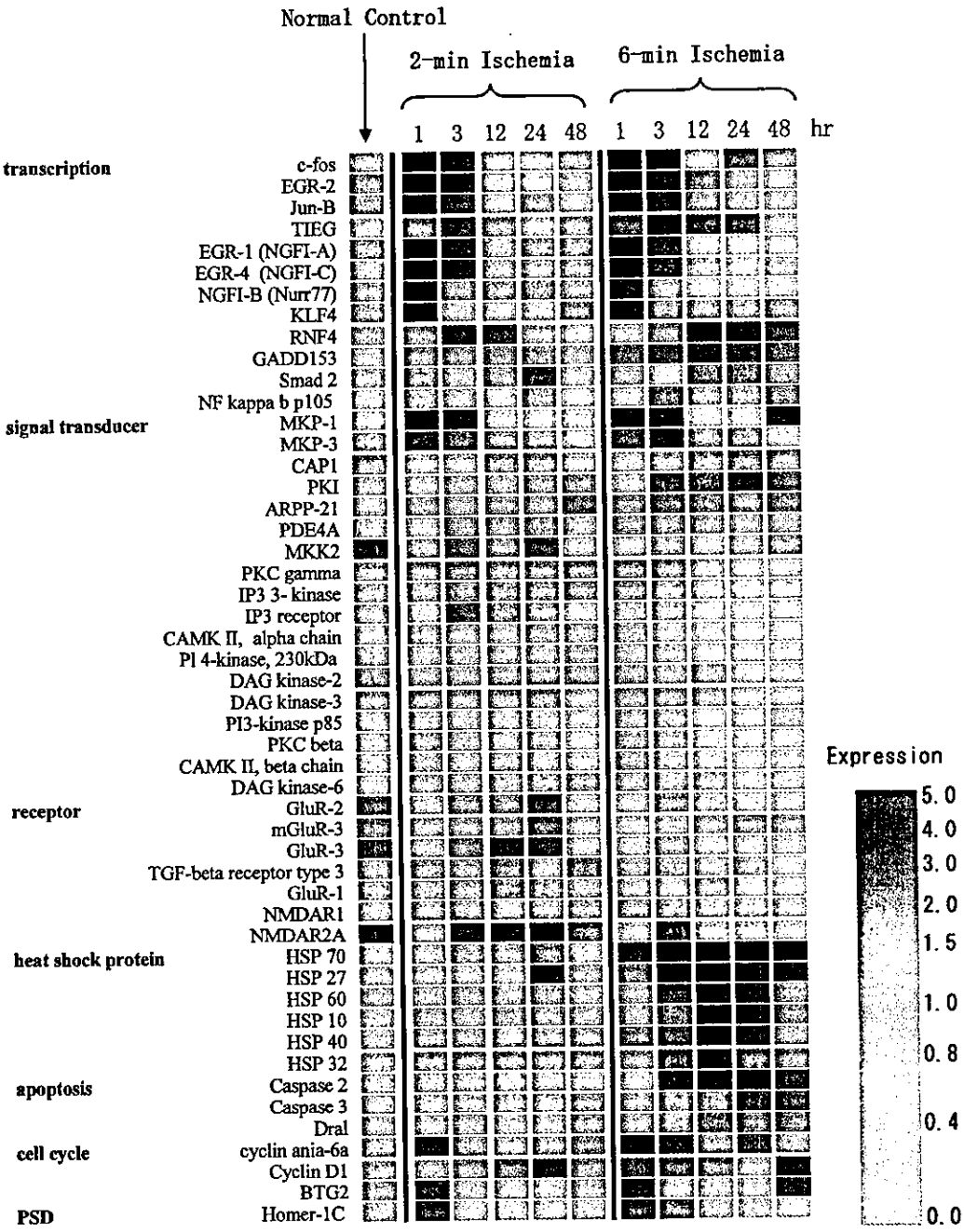

FIG. 5. Expression levels of a subset of genes described in Table. These genes are categorized into functional clusters and their expression levels are shown by color for comparison among normal control, two-minute and six-minute ischemia with time course.

1971). Thus, ischemic tolerance induced by sublethal ischemia is a suitable model for this approach, since it has been shown to be dependent on *de novo* protein synthesis (Barone et al., 1998). The most conspicuous changes we observed were for HSP70, leucine zipper and zinc finger transcription factors, such as c-Fos, JunB, Egr-1 (NGFI-A, Korx-24), Egr-2 (Krox-20), Egr-4 (NGFI-C), and a DNA-binding nuclear orphan receptor NGFI-B (Nurr77), which are regulated by a variety of stimuli or insults (for review, refer to Herdegen and Leah, 1998). Fos and Jun family members are implicated in neuronal degeneration following ischemia. In particular, c-Jun and JunB induction is observed in dying neurons after ischemia (Dragunow et al., 1994; Whitfield et al., 1999). Recently, a peptide inhibitor for c-Jun N-terminal kinase (JNK) that phosphorylates c-Jun has been shown to dramatically reduce infarction, which was accompanied by c-Jun activation and c-Fos transcription, thus indicating a critical role for AP-1 binding proteins in ischemic injury (Borsello et al., 2003). However, contra-

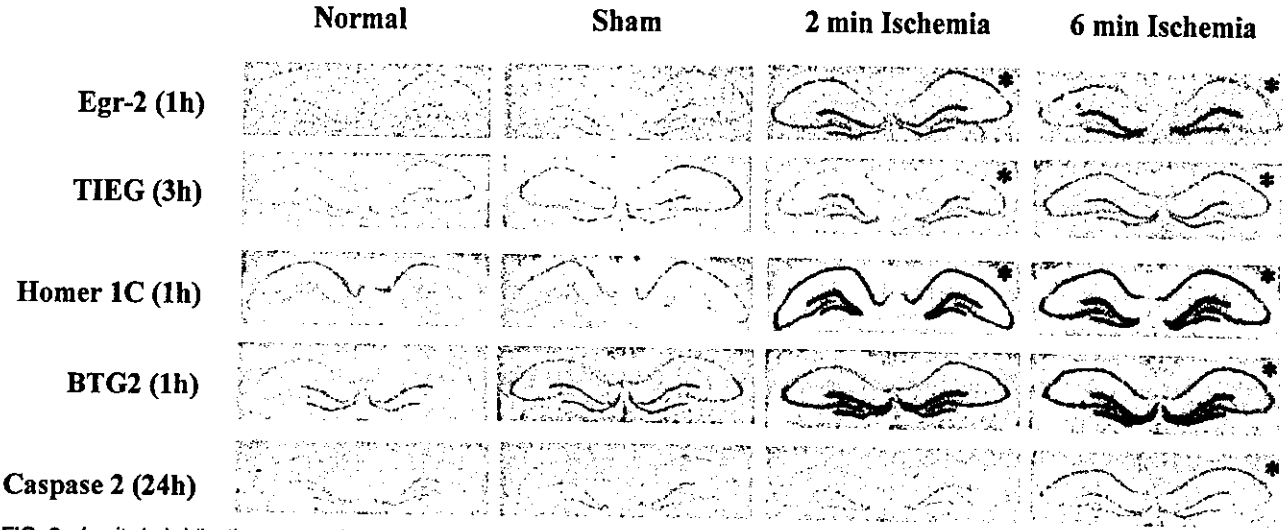

FIG. 6. *In situ* hybridization autoradiogram for Egr-2, TIEG, Homer-1C, BTG2, Caspase-2. The time-points and conditions that showed increased expression by the microarray analysis were indicated by the asterisks on the autoradiograms. Comparison between these independent methods disclosed corresponding results in four out of five genes, though the signal intensity on the CA1 sector following ischemia was equivocal for TIEG.

dictory observations have been reported that mRNA for c-Fos and JunB were widely expressed in the surviving peri-infarct area after focal ischemia (Kinouchi et al., 1994). Consistent with our observations, c-Fos and c-Jun have been shown to be up-regulated in sublethal ischemia (Sommer et al., 1995; Truettner et al., 2002) and spreading depression (Kariko et al., 1998), that renders brain resistant to ischemic injury (Kawahara et al., 1995; Kirino et al., 1991). Furthermore, hypothermia (Akaji et al., 2003) and treatment with a neuroprotective agent (Cho et al., 2001) during ischemia increased expression of c-Fos, while its attenuation by antisense oligonucleotide led to increased ischemic injury (Zhang et al., 1999). Since it is known that c-Fos and c-Jun heterodimerizations decrease the transcriptional activity of c-Jun (Herdegen and Leah, 1998), the increase in c-Fos expression may attenuate c-Jun signaling cascade to favor neuronal survival. Considering these opposing results, the effect of complex AP-1 binding protein signaling on cerebral ischemia needs to be clarified by further study.

Similarly, roles of zinc finger-transcription factors in cerebral ischemia are still controversial. For example, Egr-1 (NGFI-A, Korx-24), Egr-2 (Krox-20), Egr-4 (NGFI-C), and NGFI-B (Nurr77) were induced following focal and global ischemia (Honkaniemi and Sharp 1996; Honkaniemi et al., 1997), in which persistent expression of Egr-1 was associated with delayed neuronal death in CA1. Egr-1 and NGFI-B have been shown to induce apoptotic cell death in various *in vitro* studies (Catania et al., 1999; Li et al., 2000). However, *in vivo* evidence for a proapoptotic role in cerebral ischemia is still lacking. On the contrary, Egr-1 up-regulates the expression of antioxidant (Maehara et al., 2001) and neuroprotective EGF receptor (Nishi et al., 2002), and has been found to inhibit apoptosis following ultraviolet irradiation (Huang et al., 1998). NGFI-B has also been found to inhibit apoptosis when phosphorylated by Akt (Masuyama et al., 2001). Consistent with our findings, these observations may suggest a neuroprotective role in several contexts of insult such as sublethal ischemia.

Another important change in ischemic tolerance was robust up-regulation of MAP kinase phosphatase 1 and 3 (MKP-1 and -3). These phosphatases dephosphorylate and inactivate proteins of the mitogen activated protein kinases (MAPK) cascades (Franklin and Kraft 1997; Zhao and Zhang 2001), such as ERK (extracellular-signal regulated kinase), JNK, and p38 which play crucial roles in various stress conditions (for review, refer to Irving and Bamford, 2002). During cerebral ischemia, JNK and p38 are immediately phosphorylated (activated) and considered detrimental signals for neuronal death (Borsello et al., 2003; Gu et al., 2000; Sugino et al., 2000). Though ERK is also activated after lethal ischemia (Namura et al., 2001), its role is still controversial because it has been recently shown to be a critical pathway for induction of ischemic tolerance *in vitro* (Gonzalez-Zulueta et al., 2000), as well as *in vivo* (Gu et al., 2000; Gu et al., 2001). Of particular interest is the observation that MKP-1 is transcriptionally up-regulated and phosphorylated by ERK, leading to stabilization of the protein (Brondello et al., 1997; Brondello et al., 1999). MKP-1 is also up-regulated by hypoxia (Bernaudin et al., 2002), spreading depression, and in the peri-infarct region, which are not accompanied by neuronal injury (Gu et al., 2000; Hermann et al., 1999; Irving and Bamford 2002; Soriano et al., 2000). Since its higher

phosphatase activity is shown against JNK and p38 compared to that against ERK (Franklin and Kraft 1997), it acts rather specifically as an inhibitor of JNK and p38 signaling. Based on these findings, we speculate that MKP-1 induced by sublethal ischemia may "prime" the neurons to inhibit detrimental signals through JNK and p38 during subsequent lethal ischemic insult thus contributing to ischemic tolerance. Though this hypothesis seems attractive, it has to be verified by further *in vitro* and *in vivo* experiments at the protein level.

Compared to ischemic tolerance, remarkable changes in gene expression were associated with delayed neuronal death. However, these changes should be cautiously interpreted when considering the general translational inhibition after long lethal ischemia (Kleihues and Hossmann 1971). Nevertheless, several unique features of our study should be mentioned since some proapoptotic gene products are still increased in this condition, such as Bax and Caspase-3 (Chen et al., 1996; Chen et al., 1998), in addition to the well-described up-regulation of various heat shock proteins (Abe et al., 1998). Firstly, a substantial number of genes implicated in cell death were increased, such as NF κ b (Schneider et al., 1999), KLF4 (Chen et al., 2000), RNF4 (Pero et al., 2001), GADD153 (Murphy et al., 2001), and TGF signaling DNA biding protein Smad2 (Jang et al., 2002). Similarly, proapoptotic factors such as Caspase-2 and 3, and Dral were also increased. Caspase-2 and 3 are proteases that mediate apoptotic signals, and have already been implicated in ischemic neuronal death (Chen et al., 1998; Jin et al., 2002), whereas Dral is a newly identified gene that is p53 responsive and implicated in apoptosis (Scholl et al., 2000). Secondly, a large number of genes were down regulated. Of particular interest among these are signal transducers involved in ERK (MKK2), PI3 (PI3 kinase, PI4 kinase), and DAG/PKC (diacylglycerol kinase-2, 3, 6, PKC β and γ) pathways. Although the roles of these pathways in cell death or survival are controversial, several studies have shown their critical role as survival factors (Gu et al., 2001; Maher 2001; Marte and Downward 1997; Xia et al., 1995), which may imply attenuation of survival signals in ischemic neuronal death. PI4 kinase, a key enzyme in growth promoting PI3 kinase-Akt/PKB pathway (Marte and Downward 1997), has been shown independently to be down-regulated in ischemic neuronal death, and demonstrated to be neuroprotective when expressed persistently (Furuta et al., 2003). These observations would indicate an overall transcriptional response leading to an imbalance between death and survival signals in ischemic neuronal death, a distinctive feature not observed in ischemic tolerance.

Finally, a critical issue inherent in the current study is whether the data is reliable. We first evaluated reproducibility of housekeeping genes (GAPDH and β actin) among different arrays and confirmed that differences of expressions are within two-fold changes (data not shown). We next set the filtering value of two-fold change for duplicate samples, since this cutoff value has already been used and validated in non-tumorous expression analysis (Jin et al., 2001; Stanton et al., 2000). Another method of validation is to compare our results with those already reported in microarray analysis after ischemia (Bernaudin et al., 2002; Jin et al., 2001; Keyvani et al., 2002; Soriano et al., 2000). However, due to the differences in the model, the sampling region and timing, direct comparison is difficult. Instead, we conducted a literature search for 311 annotated genes listed in our study and identified 135 genes (43%) whose changes in expression have previously been described following ischemia in various tissues. In addition, we conducted an independent study by *in situ* hybridization, which revealed corresponding results in four out of five genes examined. However, some genes already described to be up-regulated in global ischemia did not appear in our profile, such as Bax (Chen et al., 1996). Bax transcripts exceeded the two-fold cutoff value only once in our experiments, thus failing to meet our current criteria. Though this observation may suggest low sensitivity (higher false negative rate), our results for ischemia seem to provide more specific data (lower false positive rate). Other studies also supported the reliability of oligonucleotide microarray data when compared with other validation methods, such as RT-PCR (Bernaudin et al., 2002; Tang et al., 2001), and others (Chudin et al., 2002; Ishii et al., 2000). New methods for microarray data analysis are being developed to improve sensitivity and specificity in a variety of experimental paradigms, such as Significance Analysis of Microarray Data (SAM) and Expression Deconvolution Analysis (Lu et al., 2003; Tusher et al., 2001). Further improvements and application of these methods to complex data, such as expression profiling of multiple groups along a time course, as in the current study, would improve data mining. Reinterpretation of the raw data derived from various ischemia related studies will be required in the future, using these highly sophisticated methods.

Our study revealed a wide variety of transcriptional responses with distinct patterns in relation to two different ischemic insults, namely delayed neuronal death and induced tolerance in the hippocampal CA1 region. Induced tolerance was associated with immediate and transient responses in a limited number of genes, whereas neuronal death was accompanied by immediate responses followed by delayed and long-lasting changes in a larger number of genes. Combined with changes in each gene, this genome-wide view of genomic responses will deepen our understanding of cerebral ischemia by narrowing our focus to target pathways or molecules and contribute to clarification of the molecular pathophysiology of delayed neuronal death and ischemic tolerance.

Acknowledgment: The authors thank Ms. Reiko Matsuura for technical assistance.

REFERENCES

Abe K, Kawagoe J, Aoki M, Kogure K, Itoyama Y (1998) Stress protein inductions after brain ischemia. *Cell Mol Neurobiol* 18:709–719

Akaji K, Suga S, Fujino T, Mayanagi K, Inamasu J, Horiguchi T, Sato S, Kawase T (2003) Effect of intra-ischemic hypothermia on the expression of c-Fos and c-Jun, and DNA binding activity of AP-1 after focal cerebral ischemia in rat brain. *Brain Res* 975:149–157

Barone FC, White RF, Spera PA, Ellison J, Currie RW, Wang X, Feuerstein GZ (1998) Ischemic preconditioning and brain tolerance: temporal histological and functional outcomes, protein synthesis requirement, and interleukin-1 receptor antagonist and early gene expression. *Stroke* 29:1937–1950

Bernaudin M, Tang Y, Reilly M, Petit E, Sharp FR (2002) Brain genomic response following hypoxia and re-oxygenation in the neonatal rat. Identification of genes that might contribute to hypoxia-induced ischemic tolerance. *J Biol Chem* 277:39728–39738

Borsello T, Clarke PG, Hirt L, Vercelli A, Repici M, Schorderet DF, Bogousslavsky J, Bonny C (2003) A peptide inhibitor of c-Jun N-terminal kinase protects against excitotoxicity and cerebral ischemia. *Nat Med* 9:1180–1186

Brondello JM, Brunet A, Pouyssegur J, McKenzie FR (1997) The dual specificity mitogen-activated protein kinase phosphatase-1 and -2 are induced by the p42/p44MAPK cascade. *J Biol Chem* 272: 1368–1376

Brondello JM, Pouyssegur J, McKenzie FR (1999) Reduced MAP kinase phosphatase-1 degradation after p42/p44MAPK-dependent phosphorylation. *Science* 286:2514–2517.

Catania MV, Copani A, Calogero A, Ragonese GI, Condorelli DF, Nicoletti F (1999) An enhanced expression of the immediate early gene, Egr-1, is associated with neuronal apoptosis in culture. *Neuroscience* 91:1529–1538

Chen J, Zhu RL, Nakayama M, Kawaguchi K, Jin K, Stetler RA, Simon RP, Graham SH (1996) Expression of the apoptosis-effector gene, Bax, is up-regulated in vulnerable hippocampal CA1 neurons following global ischemia. *J Neurochem* 67:64–71

Chen J, Graham SH, Nakayama M, Zhu RL, Jin K, Stetler RA, Simon RP (1997) Apoptosis repressor genes Bcl-2 and Bcl-x-long are expressed in the rat brain following global ischemia. *J Cereb Blood Flow Metab* 17:2–10

Chen J, Nagayama T, Jin K, Stetler RA, Zhu RL, Graham SH, Simon RP (1998) Induction of caspase-3-like protease may mediate delayed neuronal death in the hippocampus after transient cerebral ischemia. *J Neurosci* 18:4914–4928

Chen ZY, Shie J, Tseng C (2000) Up-regulation of gut-enriched kruppel-like factor by interferon-gamma in human colon carcinoma cells. FEBS Lett 477:67–72

Cho S, Park EM, Kim Y, Liu N, Gal J, Volpe BT, Joh TH (2001) Early c-Fos induction after cerebral ischemia: a possible neuroprotective role. *J Cereb Blood Flow Metab* 21:550–556

Chudin E, Walker R, Kosaka A, Wu SX, Rabert D, Chang TK, Kreder DE (2002) Assessment of the relationship between signal intensities and transcript concentration for Affymetrix GeneChip arrays. *Genome Biol* 3:RESEARCH0005

Dragunow M, Beilharz E, Sirimanne E, Lawlor P, Williams C, Bravo R, Gluckman P (1994) Immediate-early gene protein expression in neurons undergoing delayed death, but not necrosis, following hypoxic-ischaemic injury to the young rat brain. *Brain Res Mol Brain Res* 25:19–33

Eisen MB, Spellman PT, Brown PO, Botstein D (1998) Cluster analysis and display of genome-wide expression patterns. *Proc Natl Acad Sci* U S A 95:14863–14868

Franklin CC, Kraft AS (1997) Conditional expression of the mitogen-activated protein kinase (MAPK) phosphatase MKP-1 preferentially inhibits p38 MAPK and stress-activated protein kinase in U937 cells. *J Biol Chem* 272:16917–16923

Friddle CJ, Koga T, Rubin EM, Bristow J (2000) Expression profiling reveals distinct sets of genes altered during induction and regression of cardiac hypertrophy. *Proc Natl Acad Sci* U S A 97:6745–6750

Furuta Y, Uehara T, Nomura Y (2003) Correlation between delayed neuronal cell death and selective decrease in phosphatidylinositol 4-kinase expression in the CA1 subfield of the hippocampus after transient forebrain ischemia. *J Cereb Blood Flow Metab* 23: 962–971

Gonzalez-Zulueta M, Feldman AB, Klesse LJ, Kalb RG, Dillman JF, Parada LF, Dawson TM, Dawson VL (2000) Requirement for nitric oxide activation of p21(ras)/extracellular regulated kinase in neuronal ischemic preconditioning. *Proc Natl Acad Sci* U S A 97:436–441

Gu Z, Jiang Q, Zhang G, Cui Z, Zhu Z (2000) Diphosphorylation of extracellular signal-regulated kinases and c-Jun N-terminal protein kinases in brain ischemic tolerance in rat. *Brain Res* 860:157–160

Gu Z, Jiang Q, Zhang G (2001) Extracellular signal-regulated kinase and c-Jun N-terminal protein kinase in ischemic tolerance. *Neuroreport* 12:3487–3491

Herdegen T, Leah JD (1998) Inducible and constitutive transcription factors in the mammalian nervous system: control of gene expression by Jun, Fos and Krox, and CREB/ATF proteins. *Brain Res Brain Res Rev* 28:370–490

Hermann DM, Mies G, Hossmann KA (1999) Biochemical changes and gene expression following traumatic brain injury: Role of spreading depression. *Restor Neurol Neurosci* 14:103–108

Honkaniemi J, Sharp FR (1996) Global ischemia induces immediate-early genes encoding zinc finger transcription factors. *J Cereb Blood Flow Metab* 16:557–565

Honkaniemi J, States BA, Weinstein PR, Espinoza J, Sharp FR (1997) Expression of zinc finger immediate early genes in rat brain after permanent middle cerebral artery occlusion. *J Cereb Blood Flow Metab* 17:636–646

Huang RP, Fan Y, deBelle I, Ni Z, Matheny W, Adamson ED (1998) Egr-1 inhibits apoptosis during the UV response: correlation of cell survival with Egr-1 phosphorylation. *Cell Death Differ* 5:96–106

Irving EA, Bamford M (2002) Role of mitogen- and stress-activated kinases in ischemic injury. *J Cereb Blood Flow Metab* 22:631–647

Ishii M, Hashimoto S, Tsutsumi S, Wada Y, Matsushima K, Kodama T, Aburatani H (2000) Direct comparison of GeneChip and SAGE on the quantitative accuracy in transcript profiling analysis. *Genomics* 68:136–143

Jang CW, Chen CH, Chen CC, Chen JY, Su YH, Chen RH (2002) TGF-beta induces apoptosis through Smad-mediated expression of DAP- kinase. *Nat Cell Biol* 4:51–58

Jin K, Mao XO, Eshoo MW, Nagayama T, Minami M, Simon RP, Greenberg DA (2001) Microarray analysis of hippocampal gene expression in global cerebral ischemia. *Ann Neurol* 50:93–103

Jin K, Nagayama T, Mao X, Kawaguchi K, Hickey RW, Greenberg DA, Simon RP, Graham SH (2002) Two caspase-2 transcripts are expressed in rat hippocampus after global cerebral ischemia. *J Neurochem* 81:25–35

Kariko K, Harris VA, Rangel Y, Duvall ME, Welsh FA (1998) Effect of cortical spreading depression on the levels of mRNA coding for putative neuroprotective proteins in rat brain. *J Cereb Blood Flow Metab* 18:1308–1315

Kawahara N, Ruetzler CA, Klatzo I (1995) Protective effect of spreading depression against neuronal damage following cardiac arrest cerebral ischaemia. *Neurol Res* 17:9–16

Kawahara N, Mishima K, Higashiyama S, Taniguchi N, Tamura A, Kirino T (1999) The gene for heparin-binding epidermal growth factor-like growth factor is stress-inducible: its role in cerebral ischemia. *J Cereb Blood Flow Metab* 19:307–320

Keyvani K, Witte OW, Paulus W (2002) Gene expression profiling in perilesional and contralateral areas after ischemia in rat brain. *J Cereb Blood Flow Metab* 22:153–160

Kim YD, Sohn NW, Kang C, Soh Y (2002) DNA array reveals altered gene expression in response to focal cerebral ischemia. *Brain Res Bull* 58:491–498

Kinouchi H, Sharp FR, Chan PH, Koistinaho J, Sagar SM, Yoshimoto T (1994) Induction of c-fos, junB, c-jun, and hsp70 mRNA in cortex, thalamus, basal ganglia, and hippocampus following

middle cerebral artery occlusion. *J Cereb Blood Flow Metab* 14:808–817

Kirino T (1982) Delayed neuronal death in the gerbil hippocampus following ischemia. *Brain Res* 239:57–69

Kirino T, Tsujita Y, Tamura A (1991) Induced tolerance to ischemia in gerbil hippocampal neurons. *J Cereb Blood Flow Metab* 11: 299–307

Kirino T (2002) Ischemic tolerance. *J Cereb Blood Flow Metab* 22:1283–1296.

Kleihues P, Hossmann KA (1971) Protein synthesis in the cat brain after prolonged cerebral ischemia. *Brain Res* 35:409–418

Lee CK, Weindruch R, Prolla TA (2000) Gene-expression profile of the ageing brain in mice. *Nat Genet* 25:294–297

Li H, Kolluri SK, Gu J, Dawson MI, Cao X, Hobbs PD, Lin B, Chen G, Lu J, Lin F, Xie Z, Fontana JA, Reed JC, Zhang X (2000) Cytochrome c release and apoptosis induced by mitochondrial targeting of nuclear orphan receptor TR3. *Science* 289:1159–1164

Lockhart DJ, Dong H, Byrne MC, Follettie MT, Gallo MV, Chee MS, Mittmann M, Wang C, Kobayashi M, Horton H, Brown EL (1996) Expression monitoring by hybridization to high-density oligonucleotide arrays. *Nat Biotechnol* 14:1675–1680

Lockhart DJ, Winzeler EA (2000) Genomics, gene expression and DNA arrays. *Nature* 405:827–836

Lu P, Nakorchevskiy A, Marcotte EM (2003) Expression deconvolution: A reinterpretation of DNA microarray data reveals dynamic changes in cell populations. *Proc Natl Acad Sci U S A* 100: 10370–10375

MacManus JP, Linnik MD (1997) Gene expression induced by cerebral ischemia: an apoptotic perspective. *J Cereb Blood Flow Metab* 17: 815–832

Maehara K, Oh-Hashi K, Isobe KI (2001) Early growth-responsive-1-dependent manganese superoxide dismutase gene transcription mediated by platelet-derived growth factor. *Faseb J* 15:2025–2026

Maher P (2001) How protein kinase C activation protects nerve cells from oxidative stress-induced cell death. *J Neurosci* 21:2929–2938

Marte BM, Downward J (1997) PKB/Akt: connecting phosphoinositide 3-kinase to cell survival and beyond. *Trends Biochem Sci* 22: 355–358

Masuyama N, Oishi K, Mori Y, Ueno T, Takahama Y, Gotoh Y (2001) Akt inhibits the orphan nuclear receptor Nur77 and T-cell apoptosis. *J Biol Chem* 276:32799–32805

Murphy TC, Woods NR, Dickson AJ (2001) Expression of the transcription factor GADD153 is an indicator of apoptosis for recombinant chinese hamster ovary (CHO) cells. *Biotechnol Bioeng* 75: 621–629

Namura S, Iihara K, Takami S, Nagata I, Kikuchi H, Matsushita K, Moskowitz MA, Bonventre JV, Alessandrini A (2001) Intravenous administration of MEK inhibitor U0126 affords brain protection against forebrain ischemia and focal cerebral ischemia. *Proc Natl Acad Sci U S A* 98:11569–11574

Nishi H, Nishi KH, Johnson AC (2002) Early Growth Response-1 gene mediates up-regulation of epidermal growth factor receptor expression during hypoxia. *Cancer Res* 62:827–834

Nowak TS (1990) Protein synthesis and the heart shock/stress response after ischemia. *Cerebrovasc Brain Metab Rev* 2:345–366

Paxinos G, Watson C (1986) The rat brain in stereotaxic coordinates. San Diego: Academic Press

Pero R, Lembo F, Di Vizio D, Boccia A, Chieffi P, Fedele M, Pierantoni GM, Rossi P, Iuliano R, Santoro M, Viglietto G, Bruni CB, Fusco A, Chiariotti L (2001) RNF4 is a growth inhibitor expressed in germ cells but not in human testicular tumors. *Am J Pathol* 159: 1225–1230

Pulsinelli WA, Brierley JB, Plum F (1982) Temporal profile of neuronal damage in a model of transient forebrain ischemia. *Ann Neurol* 11:491–498

Raghavendra Rao VL, Bowen KK, Dhodda VK, Song G, Franklin JL, Gavva NR, Dempsey RJ (2002) Gene expression analysis of spontaneously hypertensive rat cerebral cortex following transient focal cerebral ischemia. *J Neurochem* 83:1072–1086

Rampon C, Jiang CH, Dong H, Tang YP, Lockhart DJ, Schultz PG, Tsien JZ, Hu Y (2000) Effects of environmental enrichment on gene expression in the brain. *Proc Natl Acad Sci U S A* 97: 12880–12884

Schneider A, Martin-Villalba A, Weih F, Vogel J, Wirth T, Schwaninger M (1999) NF-kappaB is activated and promotes cell death in focal cerebral ischemia. *Nat Med* 5:554–559

Scholl FA, McLoughlin P, Ehler E, de Giovanni C, Schafer BW (2000) DRAL is a p53-responsive gene whose four and a half LIM domain protein product induces apoptosis. *J Cell Biol* 151:495–506

Schwarz DA, Barry G, Mackay KB, Manu F, Naeve GS, Vana AM, Verge G, Conlon PJ, Foster AC, Maki RA (2002) Identification of differentially expressed genes induced by transient ischemic stroke. *Brain Res Mol Brain Res* 101:12–22

Sommer C, Gass P, Kiessling M (1995) Selective c-JUN expression in CA1 neurons of the gerbil hippocampus during and after acquisition of an ischemia-tolerant state. *Brain Pathol* 5:135–144

Song G, Cechvala C, Resnick DK, Dempsey RJ, Rao VL (2001) GeneChip analysis after acute spinal cord injury in rat. *J Neurochem* 79:804–815

Soriano MA, Tessier M, Certa U, Gill R (2000) Parallel gene expression monitoring using oligonucleotide probe arrays of multiple transcripts with an animal model of focal ischemia. *J Cereb Blood Flow Metab* 20:1045–1055

Stanton LW, Garrard LJ, Damm D, Garrick BL, Lam A, Kapoun AM, Zheng Q, Protter AA, Schreiner GF, White RT (2000) Altered patterns of gene expression in response to myocardial infarction. *Circ Res* 86:939–945

Sugino T, Nozaki K, Takagi Y, Hattori I, Hashimoto N, Moriguchi T, Nishida E (2000) Activation of mitogen-activated protein kinases after transient forebrain ischemia in gerbil hippocampus. *J Neurosci* 20:4506–4514

Tang Y, Lu A, Aronow BJ, Sharp FR (2001) Blood genomic responses differ after stroke, seizures, hypoglycemia, and hypoxia: blood genomic fingerprints of disease. *Ann Neurol* 50:699–707

Truettner J, Busto R, Zhao W, Ginsberg MD, Perez-Pinzon MA (2002) Effect of ischemic preconditioning on the expression of putative neuroprotective genes in the rat brain. *Brain Res Mol Brain Res* 103:106–115

Tusher VG, Tibshirani R, Chu G (2001) Significance analysis of microarrays applied to the ionizing radiation response. *Proc Natl Acad Sci USA* 98:5116–5121

Wang H, Zhan Y, Xu L, Feuerstein GZ, Wang X. (2001) Use of suppression subtractive hybridization for differential gene expression in stroke: discovery of CD44 gene expression and localization in permanent focal stroke in rats. *Stroke* 32:1020–1027

Whitfield PC, Williams R, Pickard JD (1999) Delayed induction of JunB precedes CA1 neuronal death after global ischemia in the gerbil. Brain Res 818:450–458

Xia Z, Dickens M, Raingeaud J, Davis RJ, Greenberg ME (1995) Opposing effects of ERK and JNK-p38 MAP kinases on apoptosis. *Science* 270:1326–1331

Zhang Y, Widmayer MA, Zhang B, Cui JK, Baskin DS (1999) Suppression of post-ischemic-induced fos protein expression by an antisense oligonucleotide to c-fos mRNA leads to increased tissue damage. *Brain Res* 832:112–117

Zhao Y, Zhang ZY (2001) The mechanism of dephosphorylation of extracellular signal-regulated kinase 2 by mitogen-activated protein kinase phosphatase 3. *J Biol Chem* 276:32382–32391

Oncogene (2004) 23, 726–734

www.nature.com/onc

STAT3 and MITF cooperatively induce cellular transformation through upregulation of c-*fos* expression

Akiko Joo[1], Hiroyuki Aburatani[2], Eiichi Morii[3], Hideo Iba[4] and Akihiko Yoshimura*,[1]

[1]*Division of Molecular and Cellular Immunology, Medical Institute of Bioregulation, Kyushu University, 3-1-1 Maidashi, Higashi-ku, Fukuoka 812-8582, Japan;* [2]*Division of Genome Science, Research Center for Advanced Science and Technology, The University of Tokyo, Komaba, Meguro-ku, Tokyo 153-8904, Japan;* [3]*Department of Pathology, Osaka University Medical School, 2-2 Yamadaoka, Suita, Osaka 565-0871, Japan;* [4]*Institute of Medical Science, The University of Tokyo, Shirokane-dai, Minato-ku, Tokyo 108-8639, Japan*

The signal transducer and activator of transcription (STAT) family proteins are transcription factors critical in mediating cytokine signaling. Among them, STAT3 is frequently activated in a number of human cancers and transformed cell lines and is implicated in tumorigenesis. However, although constitutively activated STAT3 mutant (STAT3C) leads to cellular transformation, its transformation potential such as colony-forming activity in soft-agar is much weaker than that of v-src. To identify tumorigenic factors that cooperatively induce cellular transformation with STAT3C, we screened the retroviral cDNA library. We found that the microphthalmia-associated transcription factor (MITF), an essential transcription factor for melanocyte development and pigmentation, induces anchorage-independent growth of NIH-3T3 cells in cooperation with STAT3C. Microarray analysis revealed that c-*fos* is highly expressed in transformants expressing STAT3C and MITF. Promoter analysis and chromatin immunoprecipitation assay suggested that both STAT3 and MITF can cooperatively upregulate the c-*fos* gene. In addition, the transformation of NIH-3T3 cells by both MITF and STAT3C was significantly suppressed by a dominant-negative AP-1 retrovirus. These data indicate that MITF and STAT3 cooperatively induce c-*fos*, resulting in cellular transformation.

Oncogene (2004) **23**, 726–734. doi:10.1038/sj.onc.1207174

Keywords: MITF; STAT3; c-*fos*; cellular transformation

Introduction

The signal transducer and activator of transcription (STAT) family proteins were identified in the last decade as transcription factors essential for mediating virtually all cytokine signaling (Darnell, 1997; Stark *et al.*, 1998). These proteins become activated through tyrosine phosphorylation. In addition to their central roles in normal cell signaling, recent studies have demonstrated that constitutively activated STAT signaling, especially STAT3, directly contributes to oncogenesis (Bromberg and Darnell, 2000). For example, all *src*-transformed cell lines exhibit constitutively activated STAT3 (Yu *et al.*, 1995), and dominant-negative STAT3 suppresses *src* transformation without having any effect on *ras* transformation (Turkson *et al.*, 1998). More directly, Bromberg *et al.* (1999) demonstrated that a constitutively activated form of STAT3, STAT3C, which has two substituted cysteine residues within the C-terminal loop of the SH2 domain, resulting in a spontaneous transcriptionally active dimer, causes cellular transformation scored by colony formation in soft-agar and tumor formation in nude mice. Thus, the activated STAT3 molecule by itself can mediate cellular transformation. Extensive surveys of primary tumors and cell lines derived from tumors have indicated that an inappropriate activation of STAT3 occurs at a surprisingly high frequency in a wide variety of human cancers (Bowman *et al.*, 2000). However, until now, mutations in the STAT3 gene have not been identified in these cancers, hence it remained to be determined how endogenous STAT3 is constitutively activated and what kinds of genes are involved in tumorigenicity induced by constitutively activated STAT3.

The microphthalmia-associated transcription factor (MITF) is a basic helix–loop–helix leucine zipper (b-HLH-Zip) transcription factor that plays a critical role in the differentiation of various cell types, including neural crest-derived melanocytes, mast cells, osteoclasts, and optic cup-derived retinal pigment epithelium. MITF mutations in humans produce auditory–pigmentary syndromes, such as Waardenburg syndrome type IIa and Tietz syndrome, characterized by mast cell defects, inner ear problems, and abnormal, patchy pigmentation of the hair and skin. In mice, the *mi* allele protein with the deletion of 216R in the basic region is known as a dominant-negative form through the sequestration of wild-type partners in non-DNA-binding dimmers. In addition to the complete absence of melanocytes, MITF dominant-negative mutants exhibit osteopetrosis (Kitamura *et al.*, 2002). MITF consists of at least five

*Correspondence: A Yoshimura; E-mail: yakihiko@bioreg.kyushu-u.ac.jp
Received 24 June 2003; revised 4 September 2003; accepted 5 September 2003

isoforms, including MITF-A, MITF-B, MITF-C, MITF-H, and MITF-M, and MITF-M is the melanocyte-specific type (Tachibana, 1997; Udono *et al.*, 2000; Shibahara *et al.*, 2001). MITF regulates the expression of melanocyte differentiation markers, including tyrosinase, tyrosinase-related protein, and dopachrome tautomerase (DCT), all of which are required for pigmentation (Carreira *et al.*, 2000). MITF is one of the genes involved in tumor growth and the metastasis of melanoma (Vachtenheim *et al.*, 2001, Nyormoi and Bar-Eli, 2003). However, transcriptional target genes of MITF that regulate melanoma tumorigenicity or metastasis have not yet been elucidated. Moreover, since MITF alone has low or no oncogenic activity, a cofactor(s) that cooperatively functions with MITF may be necessary for the transformation of melanocytes.

In this study, we first demonstrated that STAT3 and MITF cooperatively induce cellular transformation *in vitro*. We also identified c-*fos* as a target gene of STAT3 and MITF using microarray analysis. The induction of the c-*fos* gene is necessary for the anchorage-independent growth of NIH-3T3 cells transformed with STAT3C and MITF. Our study provides a novel role of STAT3 in melanocyte proliferation and tumor growth of melanoma.

Results

Screening for STAT3C cofactors for cellular transformation

We and others have shown that NIH-3T3 cells expressing STAT3C or wild-type STAT3, which is activated by the type C hepatitis virus (HCV) core protein, possess a colony-forming potential in soft-agar and tumorigenicity in nude mice (Yoshida *et al.*, 2002). However, the number and size of the colonies and tumor size by the expression of active STAT3 are much smaller than those of NIH-3T3 cells transformed with v-src (Bromberg *et al.*, 1999; Yoshida *et al.*, 2002). Therefore, the constitutive activation of STAT3 may not be sufficient for full transformation. With this in mind, we screened cofactors that induce full transformation in cooperation with activated STAT3 by using retrovirus cDNA transfer (Kitamura *et al.*, 1995). NIH-3T3 cells expressing STAT3C (STAT3C-3T3) were infected with the HeLa cell retroviral cDNA library (2×10^6 independent clones) and plated into soft-agar medium. After 3 weeks of incubation, two large colonies were formed and the integrated cDNAs were recovered by PCR and sequenced. One colony contained MITF cDNA with N-terminal 104 amino acids deletion compared with MITF-M (ΔN-MITF), and the other colony included full-length granulin cDNA that has been shown to induce colony formation in soft-agar in NIH-3T3 cells (Zanocco-Marani *et al.*, 1999). The ATG of the exon 3 of the MITF gene was utilized as the first AUG codon in ΔN-MITF (Figure 1a). N-terminal truncation resulted in a missing N-terminal glutamine-rich region, but ΔN-MITF retained DNA-binding and transactivation domains.

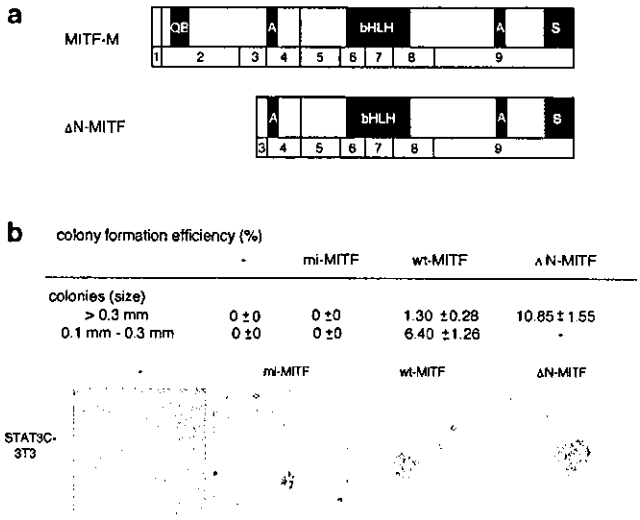

Figure 1 Transforming potential with a combination of MITF and STAT3C. (**a**) Structures of MITF-M and our screening clone, ΔN-MITF. The numbers shown under MITF isoforms indicate exons. The glutamine-rich basic region (QB), the transcriptional activation domain (A), the bHLH-LZ structure, and the serine-rich domain (S) are indicated. (**b**) STAT3C-transformed 3T3 (STAT3C-3T3) cells were infected with the pMX empty vector, pMX-mi-MITF, wt-MITF, or ΔN-MITF and plated into soft-agar medium. On day 21, colonies were counted and photographed

MITF-induced anchorage-independent growth in cooperation with STAT3C

The inserted cDNAs subcloned into the retroviral vector, pMX-IRES-EGFP, were introduced into parental NIH-3T3 cells or STAT3C-3T3 cells and then plated into soft-agar medium. N-terminal-truncated MITF induced the cellular transformation of STAT3C-3T3, but not parental NIH-3T3 cells, whereas granulin cDNA induced anchorage-independent cell growth in both NIH-3T3 cells and STAT3C-3T3 cells (Figure 1b and data not shown). Therefore, ΔN-MITF has the potential to induce the anchorage-independent growth of NIH-3T3 cells in cooperation with STAT3C. We also found that full-length (wt-) MITF could lead to anchorage-independent growth of NIH-3T3 cells in cooperation with STAT3C (Figure 1b). However, ΔN-MITF showed greater colony-forming activity, both in size and number, than wt-MITF.

We then compared the cellular morphology of transfectants. It has been reported that the forced expression of MITF in NIH-3T3 cells results in refractile cell morphology, which resembled dendritic cells and melanocytes (Tachibana, 1997). We also observed that ΔN-MITF-infected NIH-3T3 cells showed dendritic cell-like morphological changes (Figure 2a). However, as shown in Figure 2b, STAT3C-3T3 cells expressing wt-MITF or ΔN-MITF displayed some of the morphological changes associated with fibroblast transformation, that is, elongated shape and rounding.

Constitutive activation of STAT3 in melanoma cells

We then examined STAT3 activation in melanoma cells in which MITF plays an important role in transformed

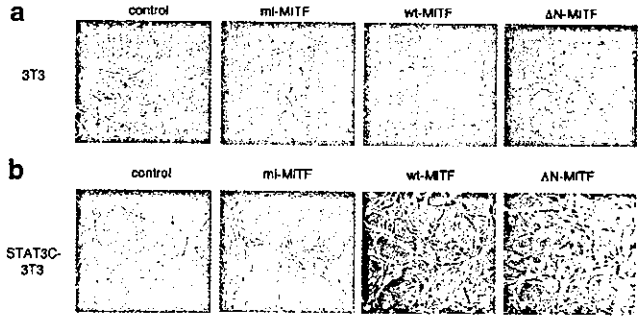

Figure 2 Cytology of MITF-infected 3T3 and STAT3C-3T3 cells. 3T3 and STAT3C-3T3 were infected with the pMX empty vector, pMX-mi-MITF, wt-MITF, or ΔN-MITF. wt-MITF and ΔN-MITF induced morphological change in both 3T3 (**a**) and STAT3C-3T3 (**b**)

phenotypes. As shown in Figure 3a, some melanoma cell lines, B16F10, G361, MMAc, and HMV-II, showed constitutive phosphorylation of STAT3. We examined whether MITF induced the constitutive activation of STAT3. Immunoblotting with an anti-phosphorylated STAT3-specific antibody revealed that phosphorylation occurred in tyrosine 705 (Y705) of STAT3 in STAT3C-3T3 cells (Figure 3b). wt-MITF and ΔN-MITF did not affect phosphorylation states of STAT3 in NIH-3T3 cells (Figure 3b). As shown in Figure 3c, MITF had little effect on or rather suppressed STAT3-dependent APRE-luciferase activity. These data indicate that STAT3 is often constitutively activated in melanoma cells, but the mechanism is probably independent of MITF expression. Furthermore, MITF-transactivation activity was not affected by STAT3C (data not shown). Therefore, we speculated that an oncogenic target gene(s) could be induced by the cooperative action of STAT3 and MITF.

Microarray screening for target genes of STAT3C and MITF

To identify target genes of MITF and STAT3, a microarray-based screen was undertaken. Total RNA was isolated from ΔN-MITF-infected NIH-3T3 (ΔN-MITF-3T3), STAT3C-3T3, and ΔN-MITF-infected STAT3C-3T3 (ΔN-MITF/STAT3C-3T3) cells and subjected to Affymetrix microarray analysis (about 12000 genes). As summarized in Figure 4a, seven genes in ΔN-MITF/STAT3C-3T3 cells were identified as more than 10-fold upregulated genes compared with ΔN-MITF-3T3 and STAT3C-3T3 cells. Most of the genes were mast cell or melanocyte-specific genes and chemokines, and the upregulation of these genes was confirmed by RT–PCR analysis (Figure 4b). Among these seven genes, the upregulation of c-*fos* is particularly interesting because c-*fos* is a component of the AP-1 transcription factor and known to be an oncogene. The functions of AP-1, composed of Fos family proteins (c-Fos, Fra-1, Fra-2, and FosB) and Jun family proteins (c-Jun, JunB, and JunD), were shown to play important roles not only in normal cell growth but also in several transformed cells induced by oncogenes (Ui *et al*., 2000). Therefore,

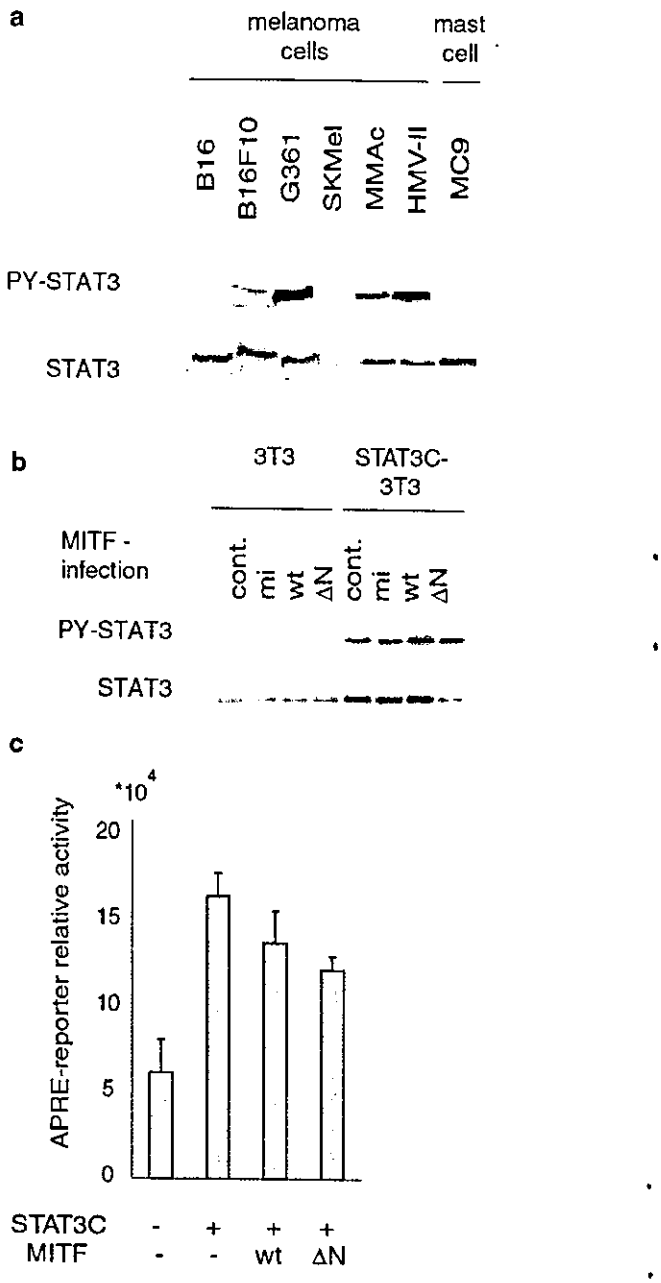

Figure 3 MITF and STAT3C do not directly activate each other. (**a** and **b**) Phosphorylation of STAT3 was detected by Western blotting with anti-phosphorylated Tyr705 of the STAT3-specific antibody. Lysate from cell lines of melanoma cells and mast cells (**a**) or 3T3 and STAT3C-3T3 cells infected with the pMX empty vector, pMX-mi-MITF, wt-MITF, or ΔN-MITF (**b**) were examined. (**c**) HEK293 cells were transfected with a plasmid mixture containing the APRE-luciferase reporter gene (0.04 μg) and the β-galactosidase gene (0.1 μg). To examine the MITF-dependent APRE-luciferase activity, cDNA of STAT3C (0.2 μg) and MITF (0.1 μg) was also introduced. Data normalized with the β-galactosidase activity from triplicate experiments are shown

we confirmed the upregulation of the c-*fos* gene by Northern blotting. As shown in Figure 4c, c-*fos* was consecutively expressed in ΔN-MITF/STAT3C-3T3 cells, but was not detected in quiescent 3T3 cells. We also detected the endogenously high expression of c-*fos*

a Target genes of ΔN MITF and STAT3C

Acc. Number	gene
L09737	GTP cyclohydrolase 1
M19681	platelet-derived growth factor-inducible protein (JE)
U14133	pmel 17
M33218	intracellular calcium binding protein (MRP-8)
M57401	mast cell protease-like protein
X70058	small inducible cytokine A7
V00727	c-fos oncogene

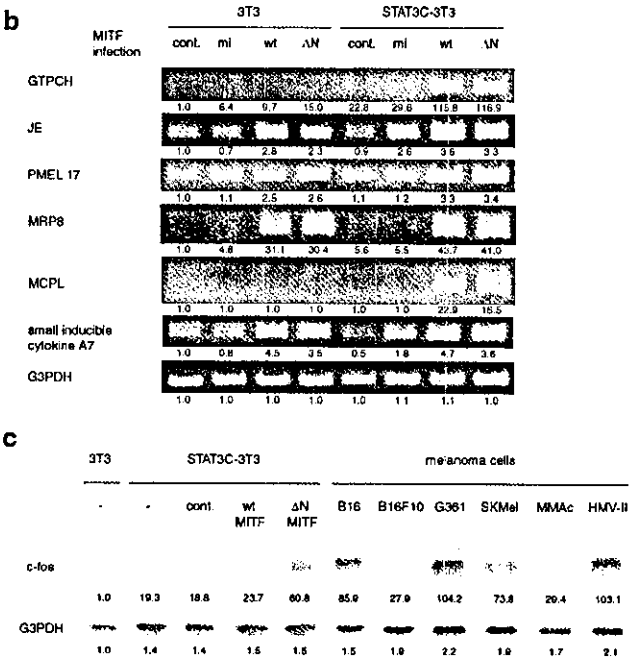

Figure 4 Expression of genes upregulated by MITF and STAT3C. **(a)** In microarray analysis, seven genes in 3T3 cells expressing both ΔN-MITF and STAT3C were found as >10-fold upregulated genes compared with STAT3C-3T3 or ΔN-MITF single transfectants. **(b)** Upregulation in six of the genes detected by microarray analysis. The mRNA expression level was evaluated by the RT–PCR method in 3T3 or STAT3C-3T3 cells infected with the pMX empty vector, pMX-mi-MITF, wt-MITF, or ΔN-MITF. The intensity of the PCR band was quantified with NIH image software. (c) Northern blotting analysis of the c-*fos* oncogene. 3T3 cells, STAT3C-3T3 cells uninfected or infected with empty vector, wt-, or ΔN-MITF viruses, and six kinds of melanoma cell lines were examined with RNA probes of c-*fos* and G3PDH

in several melanoma cell lines (Figure 4c), suggesting that the constitutive expression of c-*fos* contributes to the oncogenesis of melanoma.

STAT3 and MITF directly bind to the promoter region of c-fos

It has been shown that the c-*fos* proximal promoter region contains a single STAT3-binding site in the SIE region (Shibuya *et al*., 1994). We also noticed many MITF-binding motifs (CANNTG; E-box) (Tsujimura *et al*., 1996) in the promoter region (Figure 5a). To confirm that c-*fos* activation was cooperatively induced by MITF and STAT3C, a reporter gene assay using c-*fos* promoter luciferase constructs (Hatakeyama *et al*., 1992) was carried out. The transcriptional activity of c-*fos* was significantly increased by the transient expression of wt- or ΔN-MITF and STAT3C in HEK293 cells. MITF-induced c-*fos* promoter activation was further stimulated by leukemia inhibitory factor (LIF), which activates endogenous STAT3 (Figure 5b and data not shown).

Next, we examined the region of the c-*fos* promoter responsible for the interaction of MITF and STAT3. The c-*fos* promoter construct contains five potential MITF-binding sites. Using mutated or truncated forms of the c-*fos* promoter, we found that the SIE region is important for activation by STAT3 and an MITF-binding motif in the SRE region is essential for promoter activation by MITF (Figure 5c).

To confirm the direct binding of STAT3 and MITF to the c-*fos* promoter region, DNA-binding assay (Figure 5d) as well as chromatin immunoprecipitation (ChIP) assay (Figure 5e) were performed. First, nuclear extracts from 293T cells transfected with Myc-tagged ΔN-MITF and STAT3C or from cells stimulated with or without LIF were incubated with beads conjugated with oligonucleotides of the human c-*fos* promoter sequence, including the SIE and the SRE (55 mer). As shown in Figure 5d, MITF (lanes 2, 4, and 6) as well as both phosphorylated endogenous STAT3 (lanes 3 and 4) and STAT3C (lanes 5 and 6) bound to the oligonucleotides of the c-*fos* promoter region *in vitro*. Non-phosphorylated STAT3 without LIF stimulation (lanes 1 and 2) did not bind to the oligonucleotide beads, suggesting a specific interaction of activated STAT3 and the DNA.

For ChIP assay (Figure 5e), the crosslinked chromatins from wt-MITF/STAT3C-3T3 cells and ΔN-MITF/STAT3C-3T3 cells as well as melanomas (G361 and HMV-II) in which STAT3 was consecutively phosphorylated were immunoprecipitated with STAT3- or MITF-specific antibodies. The crosslinked protein was then removed from DNA by proteolysis. Finally, the immunoprecipitated DNA was analysed by PCR to detect the c-*fos* promoter region. As shown in Figure 5e, the anti-STAT3 antibody and the anti-MITF antibody precipitated the c-*fos* promoter SIE region and the MITF-binding motif in the SRE region, respectively.

Dominant-negative mutant of AP-1 inhibited cellular transformation of MITF/STAT3C-3T3

To investigate the contribution of the c-*fos* gene in the anchorage-independent growth of MITF/STAT3C-3T3 cells, we introduced a dominant-negative mutant of AP-1 into these cells. We used a retrovirus carrying SupJunD-1, which has an N-terminal deletion of the transactivation domain of c-Jun. We have shown that the SupJunD-1 virus suppresses the transactivation activity of AP-1 and inhibits colony formation in soft agar of various types of tumor cells (Ui *et al*., 2000). As shown in Figure 6, the dominant-negative AP-1

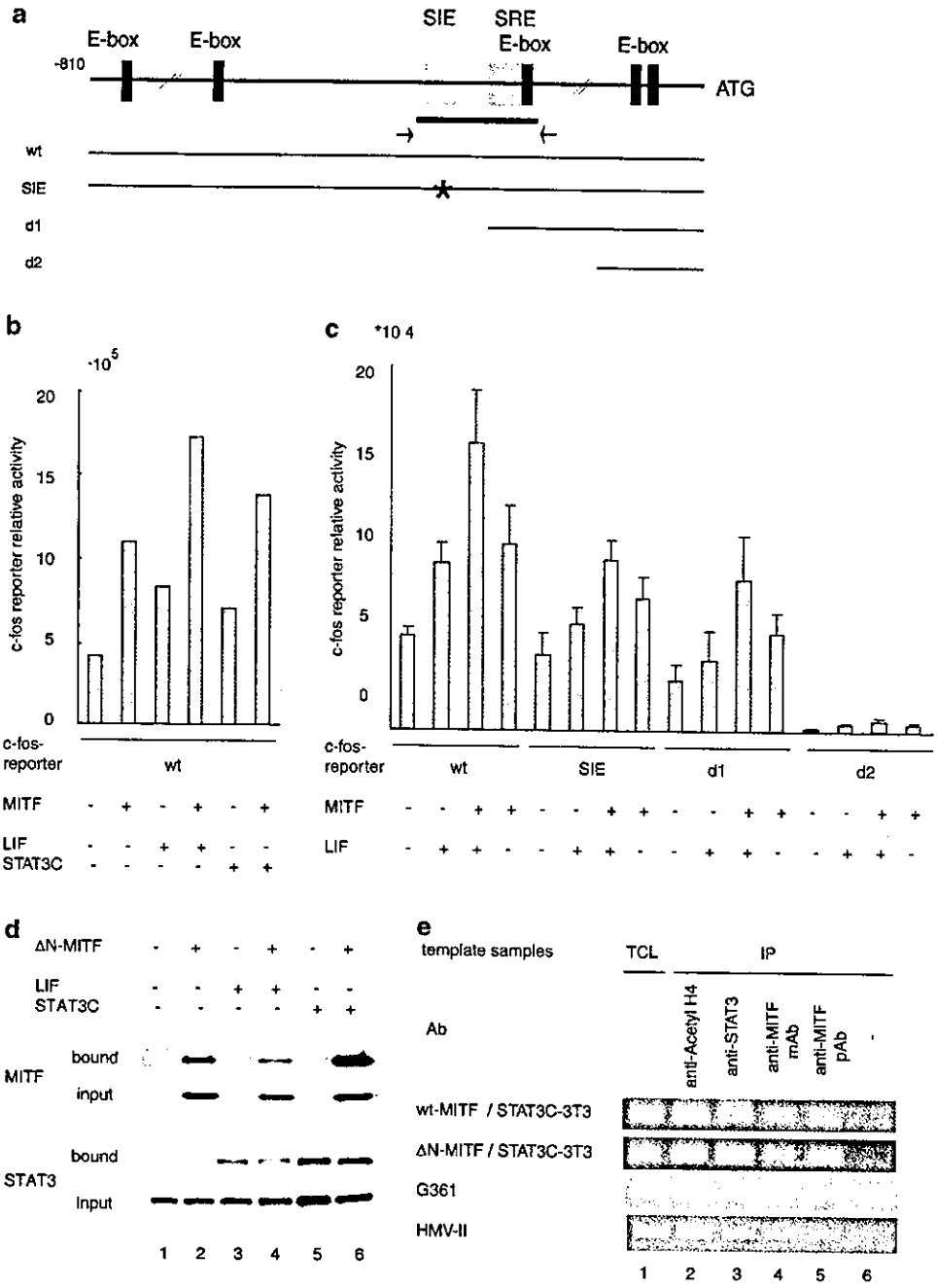

Figure 5 MITF and STAT3C directly binds to the promoter region of c-fos. (**a**) A diagram of the c-*fos*-luciferase reporter gene containing five E-boxes, potential MITF-binding motifs, and the SIE region known as a binding site of STAT3. Asterisks indicate mutations in SIE, and two deletion mutants (d1 and d2) are shown. The bold bar shows the region used for the DNA-binding assay and arrows show the PCR primers for ChIP assay. (**b** and **c**) *Reporter assay*. HEK293 cells were transfected with a plasmid mixture containing the c-*fos*-luciferase reporter gene (2 ng), the β-galactosidase gene (0.1 μg), STAT3C (0.2 μg), and the wt-MITF plasmid (**b**, 200 ng, and **c**, 10 ng). After transfection, cells were incubated in the presence or absence of 10 ng/ml LIF for 8 h, and cell extracts were prepared. Data normalized with the β-galactosidase activity from triplicate experiments are shown. (**d**) *DNA-binding assay*. 293T cells were transfected with the pcDNA3-Myc-ΔN-MITF and pRcCMV-STAT3C and stimulated with 10 ng/ml LIF for 6 h, and the nuclear extracts were prepared. The DNA-binding proteins bound to the oligonucleotide-conjugated beads were analysed by immunoblotting with anti-STAT3 and anti-Myc antibodies. (**e**) ChIP assay was performed to determine the binding of MITF and STAT3 to the promoter region of c-*fos*. wt- or ΔN-MITF-infected STAT3C-3T3 was determined *in vitro*, and the melanoma cells G361 and HMV-II were examined *in vivo*. Chromatin complexes were immunoprecipitated with anti-acetylated histone H4, anti-STAT3, and monoclonal or polyclonal anti-MITF antibodies

significantly suppressed the anchorage-independent growth of wt- or ΔN-MITF-infected STAT3C-3T3 cells. These data support our notion that c-*fos* induction is one of the mechanisms of increased anchorage-independent growth of MITF/STAT3C-expressing cells.

colony formation efficiency (%)

	retrovirus infection	wt-MITF	ΔN-MITF
colonies (size)			
> 0.3 mm	-	1.30 ± 0.28	10.85 ± 1.55
	cont.	1.11 ± 0.41	6.83 ± 3.31
	dnAP-1	0.03 ± 0.05	1.33 ± 0.90
0.1 mm - 0.3 mm	-	6.40 ± 1.26	-
	cont.	4.98 ± 1.88	-
	dnAP-1	0.84 ± 0.88	-

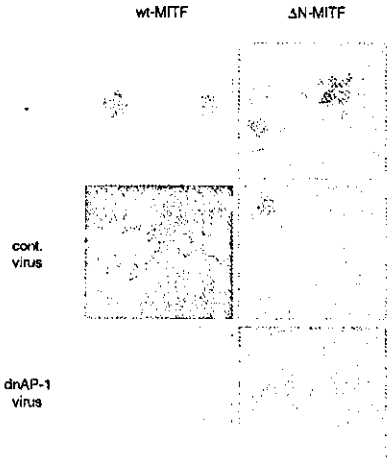

Figure 6 Expression of dominant-negative AP-1 inhibits anchorage-independent growth of MITF/STAT3C-expressing cells. wt- or ΔN-MITF-infected STAT3C-3T3 cells were infected with retrovirus carrying dominant-negative AP-1 (dnAP-1) or an empty vector by the retrovirus at moi = 10. Cells were selected with puromycin and then plated into soft-agar medium. On day 21, colonies were counted and photographed. Data from triplicate experiments are shown

Discussion

In this study, we identified MITF as a collaborative factor of STAT3 for cellular transformation. Many factors have been shown to interact with and activate (or in some cases inactivate) STAT3. For example, we have shown that the HCV core protein directly interacts with STAT3 and induces phosphorylation and activation (Yoshida *et al*., 2002). Nakayama *et al*. (2002) reported that a nuclear zinc-finger protein EZI enhances the nuclear retention and transactivation of STAT3. PIAS3 (Levy *et al*., 2002), cyclinD (Matsui *et al*., 2002), and GRIM-19 (Lufei *et al*., 2003) also interact directly with STAT3, but inhibit transcriptional activity. Most of these factors are isolated as a physical binding protein with STAT3. In this study, by using functional expression screening, we showed that STAT3 and MITF interact functionally, but not physically. A common target of STAT3 and MITF is found to be c-*fos*, which may participate in transformation by constitutively active STAT3 and MITF. Our functional cloning strategy using retroviral cDNA transfer will provide an additional candidate for the cofactor that modulates the function of STAT3. Furthermore, in this study we demonstrated that the microarray technique is a powerful tool to identify a target gene that is cooperatively induced by two distinct classes of transcription factors.

MITF consists of at least five isoforms, MITF-A, MITF-B, MITF-C, MITF-H, and MITF-M, differing at their N-termini and expression patterns (Tachibana, 1997; Udono *et al*., 2000; Shibahara *et al*., 2001). However, the clone (ΔN-MITF) we obtained from the HeLa cell library has an N-terminal deletion, which is shorter than other reported forms. Since mRNA corresponding to ΔN-MITF has not been reported, we speculate that ΔN-MITF is a product of the incomplete elongation of cDNA by reverse transcriptase. Nevertheless, ΔN-MITF seems to be a more potent inducer for a transformed phenotype of NIH-3T3 cells (Figure 1) and c-*fos* induction (Figure 4). In addition to the previously characterized acidic activation domain necessary for melanocyte differentiation, a second potential activation domain is shown to be located between amino acids 140 and 185 (Mansky *et al*., 2002), and ΔN-MITF contains these regions. Therefore, the N-terminal, with about 100 amino acids of MITF-M, may be a negative regulatory domain. This region contains a glutamine-rich basic region (QB), but the function of this region has not been elucidated. Most notably, Ser 73 of MITF-M is a predicted MAP kinase-phosphorylation site and is implicated in p300/CBP recruitment (Hemesath *et al*., 1998) and reduced MITF protein stability (Kim *et al*., 2003). Since ΔN-MITF lacks this Ser 73, dN-MITF may be more stable than wt-MITF.

Several types of functional interactions between STAT3 and MITF have been proposed. The protein inhibitor of activated STAT3 (PIAS3) has been shown to bind to a b-HLH-Zip domain of MITF, resulting in the suppression of MITF-induced transcriptional activity (Levy *et al*., 2002). However, it has been reported that STAT3 does not interfere, either *in vitro* or *in vivo*, with the interaction between PIAS3 and MITF. This finding is consistent with our data showing that STAT3 does not affect MITF transcriptional activity (data not shown) and MITF does not interfere with STAT3 transcriptional activity (Figure 3c). Recently, Kamaraju *et al*. (2002) reported that IL-6 receptor/IL-6 chimera induces a loss of melanogenesis preceded by a sharp decrease in MITF mRNA and gene promoter activity in B16/F10.9 melanoma cells. IL6RIL6 stimulates gp130, leading to the rapid activation of STAT3, which downregulates Pax3, a paired homeodomain factor regulating MITF mRNA levels and the development of melanocytes. Therefore, in this case, MITF downregulation by STAT3 is indirect, and the mechanism of Pax3 downregulation by STAT3 is not clear. The Pax3 downregulation in IL6RIL6-induced F10.9 cells leads to growth arrest and transdifferentiation to a glial cell phenotype. Therefore, the genetic interaction between MITF and STAT3 seems to be complicated and probably different among cell types.

We found that the c-*fos* gene is a common target of STAT3 and MITF, which probably contributes to transformation. Microarray analysis also revealed that